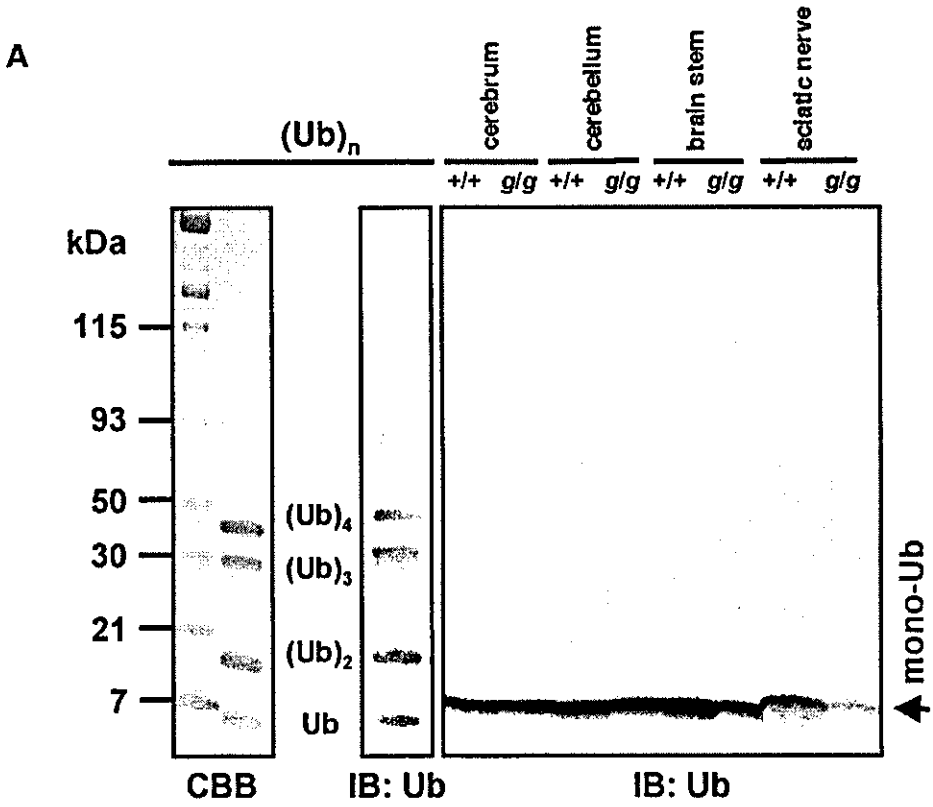

Figure 3. Loss of UCH L1 decreases the level of monoubiquitin. (**A**) A mixture of 1 μg ubiquitin and 4 μg poly-Ub was subjected to SDS–PAGE and stained with coomassie brilliant blue (left panel). Ten percent of this mixture was electrophoresed and immunoblotted with a monoclonal antibody to Ub (Chemicon) that recognizes both conjugated and unconjugated mono-/poly-Ub in denatured states (middle panel). Cytosolic fractions (20 μg) from various neuronal tissues of wild-type and *gad* mice were immunoblotted using the same antibody (right panel). (**B**) Levels of free mono-Ub in cytosolic (upper) and the nuclear (lower) fractions were measured by radioimmunoassay (16) in various brain structures from mice less than 2 weeks old ($n = 5$ for cerebrum, cerebellum and brain stem; $n = 4$ for sciatic nerve). Mean values with SEM are shown as open (+/+), gray (+/−) or black (*g/g*) bars. $^{**}P < 0.01$; $^{*}P < 0.05$.

adeno-*Uch l1* transfected cell to β-*gal*-transfected cell were 2.3 ± 0.2 to bands corresponding to mono-Ub and 1.5 ± 0.2 to bands corresponding to MW50-115; $n = 3$, corrected by β-actin).

Next, mice carrying a *Uch l1* transgene under control of the EF-1α promoter were generated (Fig. 5A). These mice exhibit no apparent neurological phenotype during life. However, transgenic (Tg) mouse expressing a high copy number of

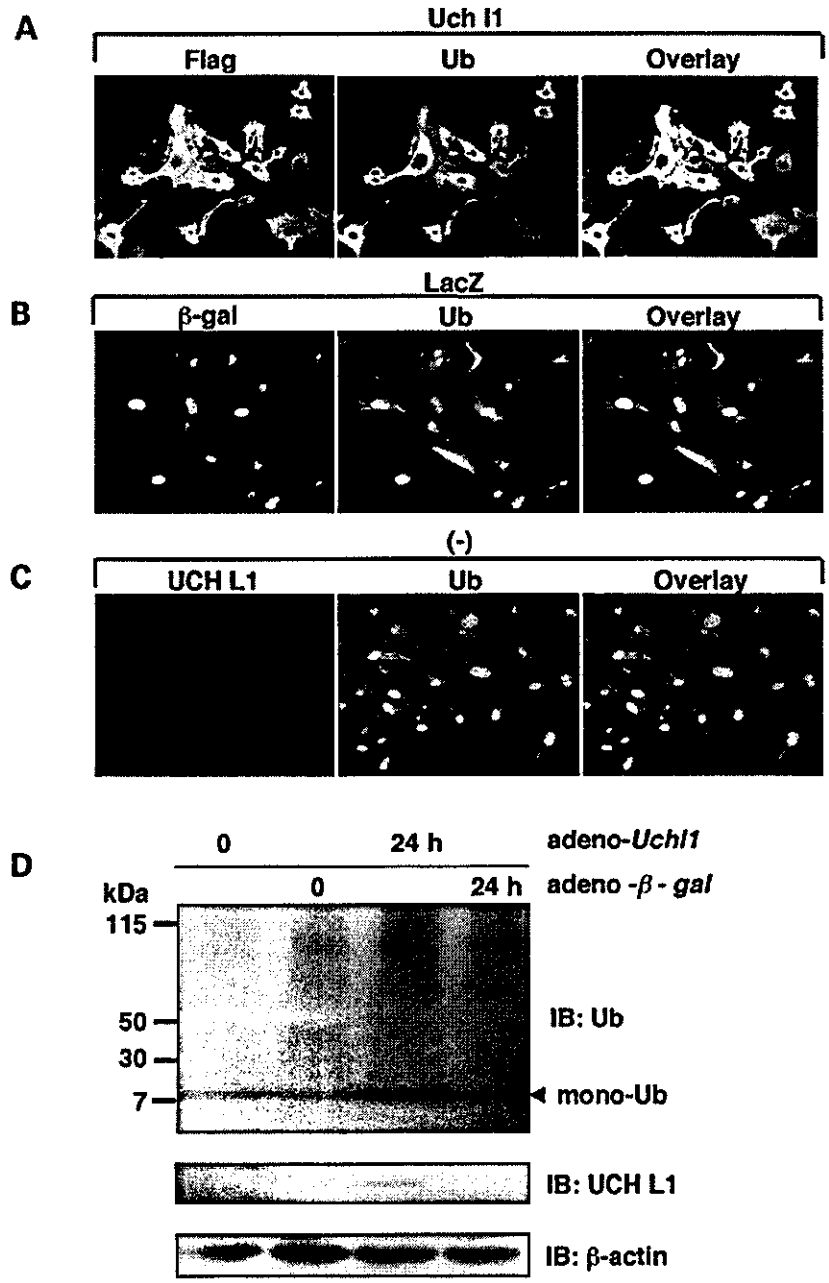

Figure 4. Overexpressed UCH L1 co-localizes with ubiquitin and increases ubiquitin levels in cultured cells. (A–C) E13.5 primary mouse embryonic fibroblasts (MEF) cells were transfected with adenovirus vectors expressing either *Uch l1* (A) or β-gal (B) or not transfected (C). UCH L1 was induced using Cre recombinase for 24 h. Antibodies to flag-tag and β-gal were used for immunostaining to exogenic UCH L1 and β-gal (A, B; left panels). An absence of immunoreactivity to anti-UCH L1 showed the lack of endogenous UCH L1 expression in MEF cells (C; left panel). MEF cells were also labeled with polyclonal anti-Ub (Sigma; A–C; middle panels). Immunoreactivities to anti-Ub/-UCH L1 completely merge in MEF cells transfected with adeno-*Uch l1* (A; right panel), but not in cells transfected with β-gal (B; right panel) and not transfected (C; right panel). Ub localization appears to be recruited to the UCH L1. (D) Cell lysates were immunoblotted with anti-Ub (Chemicon) or anti-UCH L1 at the indicated times (upper and middle panels). The same membrane was re-blotted with an antibody to β-actin (lower panel). Band intensities were measured at the bands corresponding to mono-Ub and poly-ubiquitinated bands at MW50-115 kDa and normalized by β-actin intensities.

foreign DNA and high-level of mRNA from *Uch l1* transgene were all infertile ($n = 6$, manuscript in preparation). Therefore, we examined two of these infertile Tg mice, 11 and 22 (Fig. 5B). Immunohistochemistry of brain sections showed increased levels of UCH L1 immunoreactivity in the nervous system of Tg mice (Fig. 5C; left panel, cerebral cortex; right panel, cerebellum). The antibody to Ub that preferentially stains free mono-Ub showed a significant increase in Ub immunoreactivity in Tg mice (Fig. 5D; cerebellum). Immunoblotting also showed the increased level of mono-Ub in Tg mice (Fig. 5E; band intensity for mono-Ub of Tg 22 to wild-type was 2.3 in cerebrum and 1.5 in cerebellum). These data show that UCH L1 overexpression increases the level of mono-Ub in the cultured cells and nervous system *in vivo*.

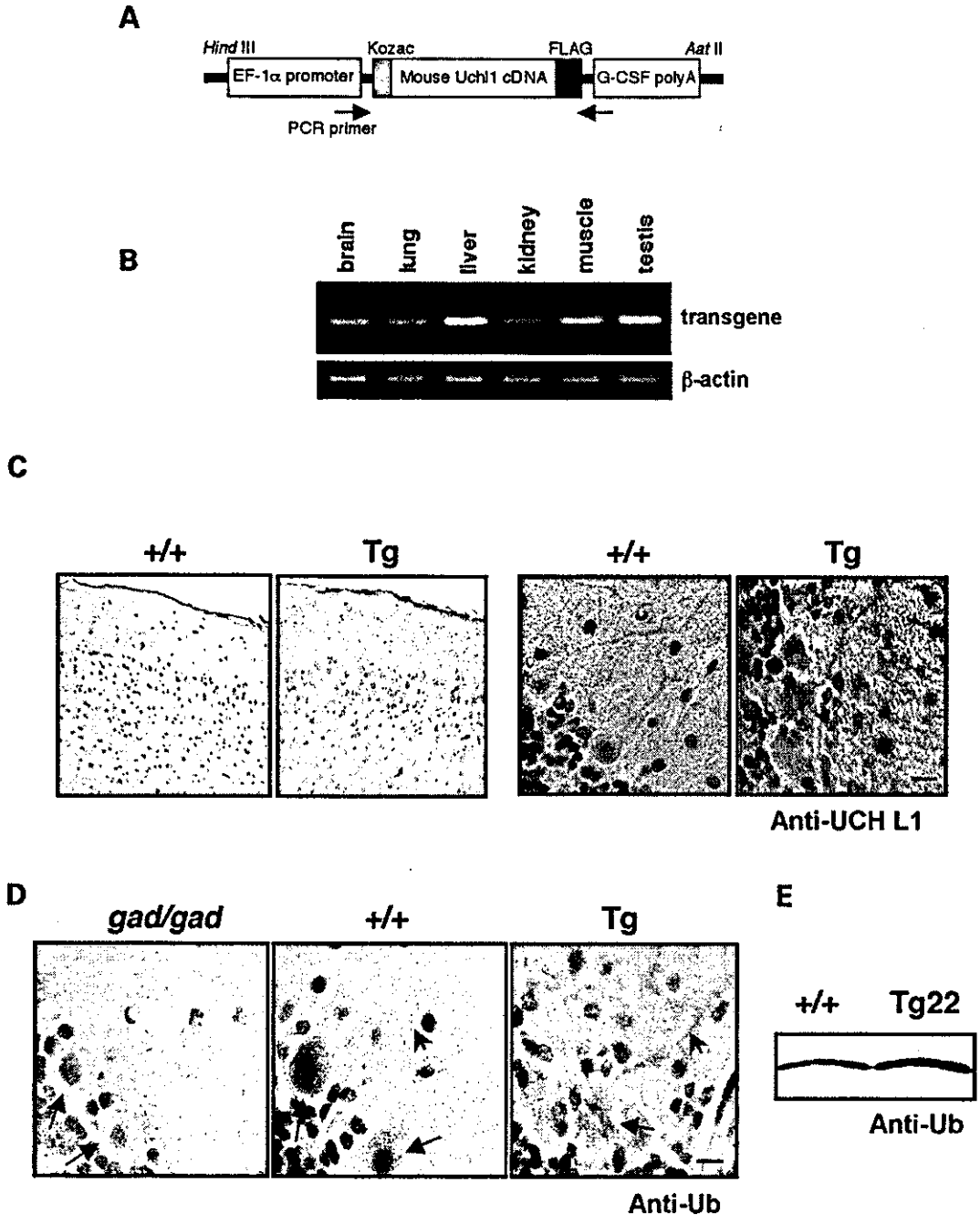

Figure 5. UCH L1 overexpression increases ubiquitin level in the mouse nervous system. **(A)** Construction of the transgenic vector. Flag-tagged mouse *Uch l1* cDNA was subcloned into pEF-Bos vector that carries EF-1α promoter. **(B)** Total RNAs of 5 μg from various organs of transgenic (Tg) mouse 22 were subjected to RT–PCR using specific primers to transgenic *Uch l1* cDNA (upper panel) and β-actin (lower panel). **(C)** Immunohistochemisty to anti-UCH L1 antibody to cerebral cortex (left panels) and cerebellum (right panels) from Tg 22 and wild-type mouse. Scale bars, 20 μm. **(D)** Cerebellar sections from *gad* (*gad/gad*), wild-type (+/+), and UCH L1 transgenic mice (Tg 22) brains were analyzed by immunohistochemistry using polyclonal anti-Ub (Sigma) as the primary antibody. Ub reactivity was increased in Tg 22 mouse. The *gad* mouse showed decreased immunoreactivity to anti-Ub. Arrows and arrowheads indicate Purkinje cell body and neurites, respectively. Scale bars, 20 μm. Twenty micrograms of proteins of the cerebrum **(E)** and cerebellum from Tg 22 and wild-type mouse were subjected to SDS–PAGE and immunoblotted with anti-Ub.

Mechanism by which UCH L1 increases Ub levels

The basis of the UCH L1-mediated increase in Ub levels was examined using three different approaches. First, Ub transcriptional regulation was examined in both wild-type and *gad* mice. The mRNA levels of all four Ub genes, *Uba52*, *s27a*, *UbB* and *UbC*, were analyzed by quantitative PCR but no significant differences were observed between wild-type and *gad* mice (Fig. 6A). A reporter assay using the *UbC* gene promoter also showed no effect of UCH L1 on

transcriptional activation of the *UbC* gene (Fig. 6B). These experiments showed that UCH L1 does not upregulate Ub levels via transcriptional activation.

Second, to address the possibility that a reduction in the release of mono-Ub from poly-Ub or Ub-conjugated proteins affects the level of free mono-Ub in *gad* mice, UCH L1-catalyzed release of mono-Ub from substrates was tested. UCHs can generate mono-Ub from poly-Ub and peptide–ubiquityl amides *in vitro* (12). However, no enhanced intensity corresponding to the release of Ub from poly-Ub (Fig. 3A; compare left and right panels) or mass spectra corresponding to the hydrolysis of peptide–ubiquityl amides (Fig. 1E) was observed in the *gad* mouse immunoprecipitates from brain lysates. Alternatively, an unknown substrate could be upregulated as poly-Ub-conjugated proteins (multi-Ub) in *gad* mice. Therefore, multi-Ub levels were measured in soluble mouse brain lysates by sandwich ELISA using antibody FK2 that is specific for multi-Ub (16–18) (Fig. 6C). No difference in the level of multi-Ub was observed between the wild-type and the *gad* mouse at less than 2 weeks of age. These data argue against the hypothesis that the deficiency in UCH L1-catalyzed release of mono-Ub from multi-Ub is responsible for the decreased level of Ub observed in the *gad* mouse.

Third, the effect of UCH L1 expression on Ub metabolism was examined in MEF cells transfected with either adeno-*Uch l1* or -β-*gal*. Mono-Ub levels were monitored for 30 h after pulse-chase labeling and Ub degradation was compared by autoradiography. Ub half-life was extended in MEF cells transfected with UCH L1 (Fig. 6D). Since lysosomes are implicated as the site of Ub degradation, we examined the effect of the lysosomal inhibitor EST (2,3-*trans*-epoxysuccinyl-L-leucylamide-3-methyl butane ethyl ester) on Ub metabolism (19,20). EST extended Ub half-life in both adeno-*Uch l1*- and adeno-β-*gal*-transfected MEF cells (Fig. 6D) and, under these conditions, mono-Ub degradation was comparable between the adeno-*Uch l1*-transfected cells and the control cells (Fig. 6D).

These data suggest that UCH L1 affects Ub degradation and alters its metabolism, and that Ub degradation occurs in lysosomes.

UCH L1 affinity for Ub appears to be indispensable for the maintenance of Ub levels

To further clarify the effect of UCH L1 on Ub levels, his-tagged *Uch l1* and mutants were transfected into dopamine-producing SH-SY5Y neuronal cells (Fig. 7). UCH L1 and Ub were then visualized using confocal immunofluorescence microscopy. Cells transfected with wild-type *Uch l1* showed a relative increase in Ub immunoreactivity compared with mock-transfected cells (anti-Ub; Sigma, polyclonal; Fig. 7A and E) consistent with Ub upregulation by UCH L1. *Uch l1*^{I93M}, implicated in the pathogenesis of PD, also increased Ub immunoreactivity comparable to wild-type *Uch l1* (Fig. 7B and E). Increased Ub immunoreactivity was also evident in cells transfected with *Uch l1*^{C90S}, which retains Ub binding affinity but lacks C-terminal hydrolase activity (Fig. 7C and E; Table 1) (9). However, significant increase in Ub immunoreactivity was not observed with mutant *Uch l1*^{D30K} (Fig. 7D and E), which carries a charge reversal on the surface of the protein that is presumed to interact with cationic residue of Ub (21). This mutant protein exhibits markedly lower affinity for Ub and has no hydrolase activity (Table 1). These data suggest that UCH L1-mediated increases in Ub levels are a function of UCH L1 affinity for Ub rather than hydrolase activity.

DISCUSSION

In spite of the abundance of UCH L1 in the nervous system and its importance in the neurodegenerative diseases, the *in vivo* functions of UCH L1 have been remained unknown (6–13). The *gad* mouse and the UCH L1 transgenic mouse revealed a novel role for UCH L1 in neurons. Our data indicate that UCH L1 is associated with mono-Ub and elevates the level of mono-Ub in neuron. Previously, Doa4, a deubiquitinating enzyme belonging to UBPs, was reported to elevate the level of Ub in yeast, although the association of Doa4 with Ub was not mentioned (19). From a genetic complementation study, Doa4 was inferred to be involved in endosomal–lysosomal pathway (20). Our pulse-chase labeling using MEF cells suggests that UCH L1 affects Ub metabolism and extends its half-life by inhibiting Ub degradation. As an inhibitor of lysosomal function extended Ub half-life and partially diminished the effect of UCH L1, UCH L1 probably prevents Ub degradation in lysosomes. Thus, our results also suggest the link of DUBs to the endosome–lysomal pathway. Recently, it was demonstrated that Ub itself contains all the necessary signals for both targeting and degradation of monoubiquitylated proteins in the endosomal–lysosomal pathway, with the crucial Ub residues being Gln2, Phe4, Lys6, Leu8, Val26, Leu43, Ile44, Glu64 and Val70 (22,23). Possibly some fraction of free Ub itself is shunted into the endosome–lysosomal pathway and UCH L1 binding to Ub may suppress this route by masking Ub residues that are requisite for targeting. Alternatively, it may be possible that UCH L1 deubiquitylates ubiquitylated proteins before degradation within the endosome–lysosome pathway. However, UCH L1^{C90S}, lacking hydrolase activity, still retains the ability to maintain Ub levels, suggesting that physical association with UCH L1 rather than its deubiquitylating activity promotes Ub stability. Although UCH L1 can very slowly cleave poly-Ub and Ub-small molecule adducts *in vitro* (4), we did not find accumulation of such Ub species in *gad* mice. This finding may reflect functional redundancy between UCHs and UBPs. Alternatively, such Ub species may be detergent insoluble and exist within aggregates of Ub in dot-like structures observed in *gad* mice (10).

It has been long known that Ub-containing protein aggregates as hallmarks of various neurodegenerative conditions (2). Such aggregates are remnants of inadequate proteolysis and suggest either surpluses of aggregation-prone abnormal proteins or insufficiencies in Ub-dependent proteolysis (Fig. 8). PD caused by A53T and A30P mutations of α-synuclein appear to be the examples for the former case. These mutant proteins are more stable than wild-type and presumed to surpass the critical concentration of α-synuclein for oligomerization (24,25). The latter case appears to account for both a *Uch l1* gene deletion in the *gad* mouse and the parkin gene mutations in the patients with PD. Loss of function mutations in Parkin E3 ligase may prevent this enzyme from properly ubiquitylating putative

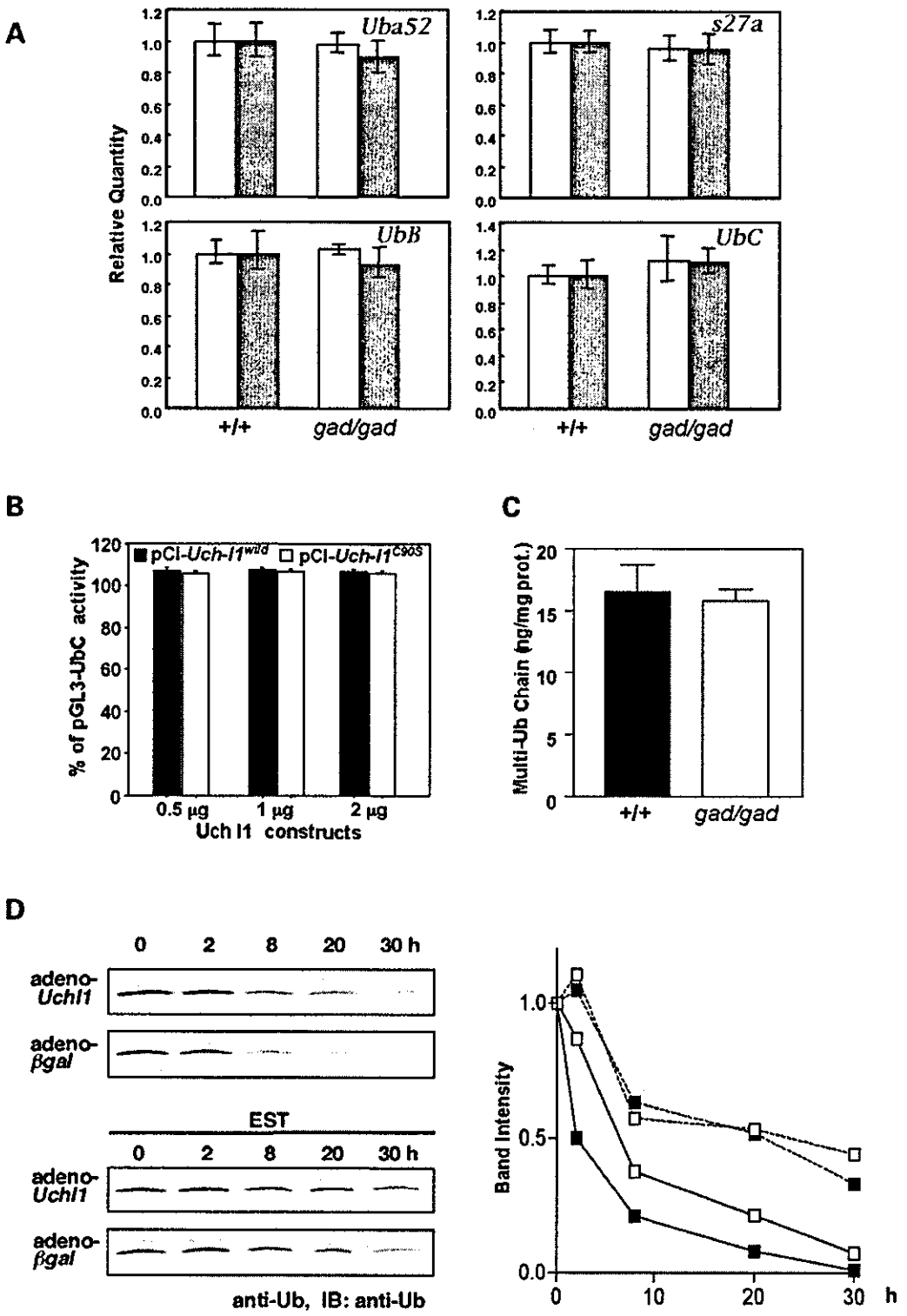

Figure 6. Effects of UCH L1 on transcription, processing and post-translational state of ubiquitin. (**A**) Quantitative RT–PCR for *Uba52*, *s27a*, *UbB* and *UbC* was performed using total RNA from wild-type and *gad* (*gad/gad*) cerebrum ($n = 3$). Mean values are shown with SEM. β-Actin (open bar) or GAPDH (solid bar) were used as internal controls. (**B**) Dual luciferase assay of a vector containing the +18 to +1227 bp region of the human Ub C promoter (pGL3-*UbC*) co-transfected with either UCH L1 (pCI-neo-$Uchl1^{WT}$; solid bar) or an active site mutant of UCH L1 (pCI-neo-$Uchl1^{C90S}$; open bar). Mean values from eight independent experiments are shown with SEM. (**C**) Levels of multi-Ub chain (conjugated poly-Ub) in cerebellum cytosolic fractions were measured by ELISA from 2-week-old mice ($n = 6$) (16–18). Mean values with SEM are shown as filled (+/+) or open (*gad/gad*) bars. (**D**) Adeno-*Uchl1*-transfected or adeno-β-*gal*-transfected MEF cells were labeled with [^{35}S]-Met. Autoradiograms of anti-Ub immunoprecipitates pulse-chased at the indicated times in the absence (left upper panels) or presence of EST (2,3-*trans*-epoxysuccinyl-L-leucylamide-3-methyl butane ethyl ester; left lower panels) are shown. Relative band intensities are quantified and mean values of two independent experiments are shown (right).

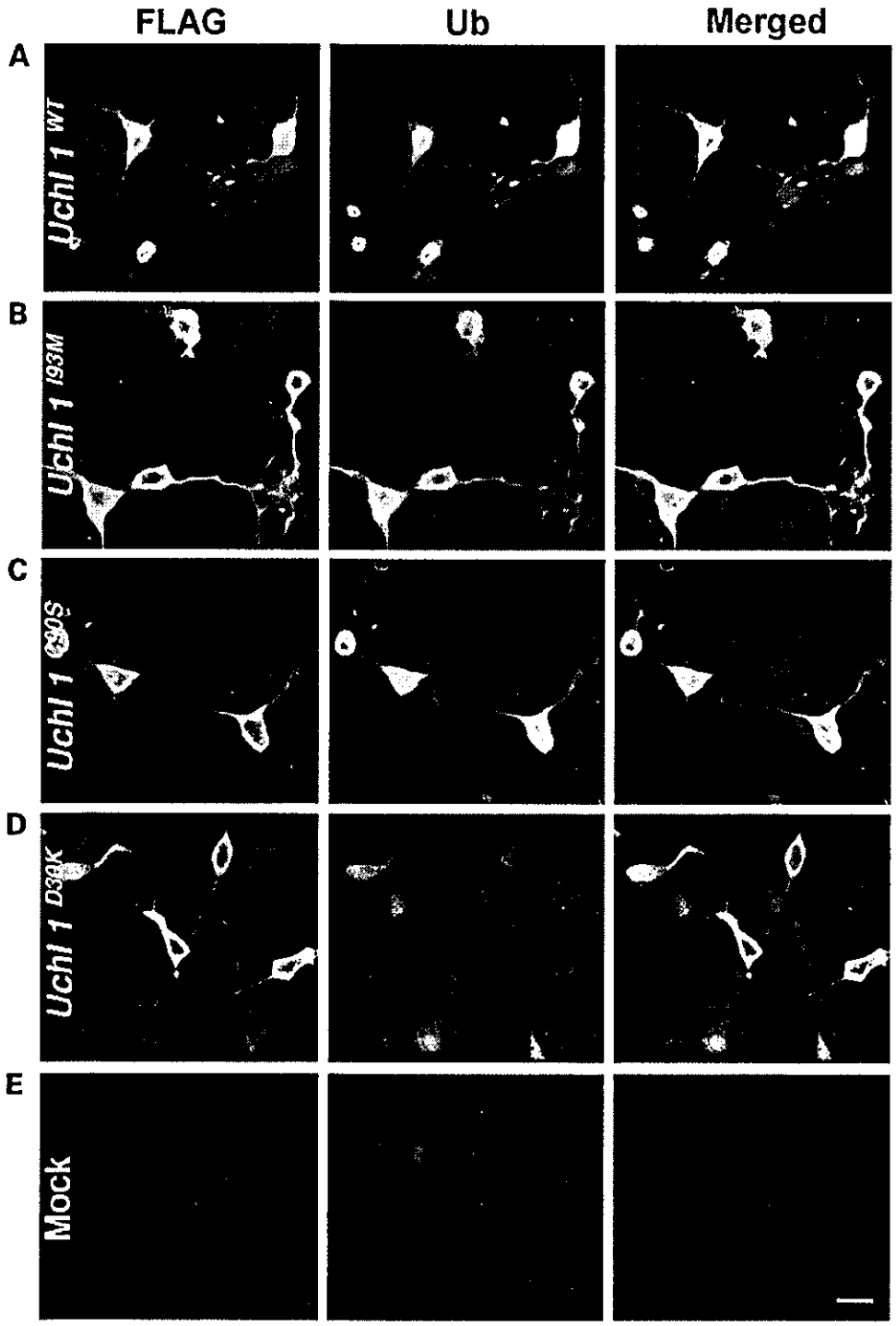

Figure 7. Effect of UCH L1 mutants on ubiquitin expression. Plasmids pcDNA3-*Uchl1*^{WT} (**A**), -*Uchl1*^{I93M} (**B**), -*Uchl1*^{C90S} (**C**), -*Uchl1*^{D30K} (**D**) and vector alone (**E**) were transfected into SH-SY5Y cells and expressed. Antibodies against flag-tag and Ub (Sigma, polyclonal) were used to detect transfected UCH and endogenous Ub, respectively. The faint green staining (left panels) reflects non-specific staining of cells that escaped transfection. Scale bars, 20 μm.

substrates (26,27), causing substrate accumulation and toxicity to neurons at the substantia nigra. Loss of functional UCH L1 could also lead to inadequate ubiquitylation via decrease of free Ub. An initial pathological lesion begins at the synapse of the sciatic nerve in the *gad* mouse. Ub is known to be transported over long distances via slow axonal transport to synapse (28). Ub decrease and the consequent inadequate ubiquitylation of proteins may trigger increased levels of proteins that should undergo Ub-dependent degradation, resulting in the accumulation of such proteins within spheroids observed in *gad* mice (11). The *gad* mouse phenotypes resemble those of Charcot–Marie–Tooth diseases (CMT) in humans. Although there are no

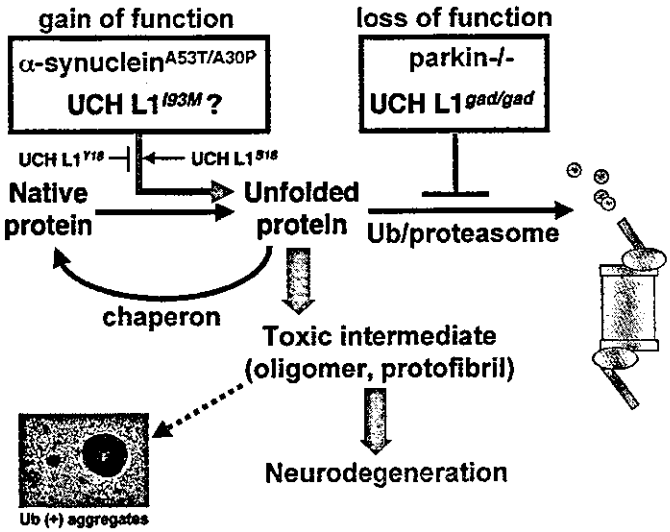

Figure 8. Common pathway of neurodegeneration. Unfolded proteins are refolded by molecular chaperons or degraded by the ubiquitin/proteasome pathway. The red boxes illustrate that excessive production of insoluble proteins by genetic defect (such as A53T/A30P mutations of α-synuclein in Parkinson's disease) or insufficiencies in the ubiquitin/proteasome pathway (such as *Uch l1* gene deletion in the *gad* mouse and the parkin gene mutations in the patients with PD) alter the proportion of denatured proteins within the cell. The accumulation of a toxic intermediate (oligomer or protofibril) is proposed to precede and promote neurodegeneration.

CMT or peripheral neuropathies that map to the proximity of the human *UCH L1* locus so far, immunohistological profiling of UCH L1 and Ub in peripheral nerves would be helpful in delineating a human *gad* analog.

Human *UCH L1* deletion mutants have not been reported although polymorphism and missense mutations of UCH genes are linked to PD (29–32). In idiopathic PD, particularly of Japanese or Chinese origin, UCH L1 gene polymorphism at position 18 is linked to a disease susceptibility (29–32). The S18Y mutation is common in Japanese and Chinese compared with Europeans and is reportedly protective for PD (19–32). Recently, UCH L1 was found to exhibit dimerization-dependent ubiquityl ligase activity at Lys63 of acceptor Ub molecules *in vitro* (13). Polyubiquitylated proteins linked to Lys48 of Ub are destined for proteasomal degradation, while those linked to Lys63 of Ub are stable. The protective variant Y18-UCH L1 exhibits diminished dimerization and ligase activities relative to S18-UCH L1, and therefore Y18-UCH L1 is predicted to accelerate degradation of proteins such as α-synuclein by making less stable species conjugated to Lys 63 of Ub. Thus, the decreased susceptibility to PD in individuals carrying the S18Y mutation could be explained by the low concentration of α-synuclein, which is yet confirmed *in vivo* (13) (Fig. 8). The I93M mutation in UCH L1 is reported in familial PD with dominant inheritance (9). α-Synuclein (dominant form) or the of parkin or DJ-1 (recessive forms) may also cause familial PD (33–35). The glycosylated form of α-synuclein is a substrate for parkin (36). Our present data indicate that UCH L1 upregulates Ub levels *in vivo*, and therefore UCH L1, parkin and α-synuclein appear to be interrelated with respect to Ub and ubiquitylation pathways. As with α-synuclein, the loss of UCH L1 function does not appear to cause PD (11,37). In patients carrying the UCH L1 mutation I93M, both ligase and hydrolase activities are presumed to be partially reduced (9,13). Our data show that UCH $L1^{I93M}$ enhances Ub immunoreactivity similar to UCH $L1^{WT}$ in transfected cells. Moreover, we did not find evidence for nigrostriatal dopaminergic pathology in either *gad* mouse heterozygotes or homozygotes. Therefore, an as yet unknown 'gain of toxic function' condition may underlie PD in patients carrying UCH $L1^{I93M}$ (Fig. 8).

Our results reveal that the fundamental defects in the *gad* mouse are due to a lack of UCH L1 and consequent Ub decrease. Ub and Ub-dependent proteolysis are involved in nearly all cellular processes and therefore it is likely that *gad* mice exhibit a wide variety of neuronal malfunctions that are not recognized by routine histology. Thus, in light of our present data we are currently re-evaluating *gad* mouse phenotypes including behavior, neuronal regeneration and apoptosis. These studies will broaden our understanding of the role of Ub pathways in neuronal function and neurodegenerative disorders.

MATERIALS AND METHODS

Plasmid and protein purification

Sequences encoding UCH L1 were amplified from a mouse brain cDNA library by polymerase chain reaction (PCR), and subcloned into either pQE-30 (Qiagen, Valencia, CA, USA) or pcDNA3 (Invitrogen, Groningen, The Netherlands) for expression in *E. coli* (for protein purification) or mammalian cells (for transfection), respectively. cDNA encoding UCH $L1^{gad}$ was obtained from a *gad* mouse brain by PCR. Another UCH L1 mutations were introduced by PCR-based site-directed mutagenesis (QuickChange Site-Directed Mutagenesis Kit, Stratagene, La Jolla, CA, USA) of template plasmids using primers designed to introduce specific mutations (D30K, C90S, I93M). Proteins overexpressed in *E. coli* were purified using Ni-agarose (Qiagen) as per the manufacturer's protocol and purified further by gel filtration using a Hi Load™ 16/60 Superdex 75 column (Amersham Pharmacia, Uppsala, Sweden).

Generation of adeno-vectors, antibodies and Ub level determination

Recombinant plasmids containing adeno-*Uch l1* and -β-*gal* were constructed using the Adenovirus Expression Vector Kit as per the manufacturer's instructions (Takara, Tokushima, Japan). Briefly, *Uch l1-flag* and β-*gal-flag* genes were inserted individually into the cosmid vector pAxCANLw containing the CAG promoter, the stuffer sequence and two loxP sequences. These recombinant cosmids were co-transfected into HEK 293 cells with a restriction enzyme-digested adenovirus DNA-TPC to generate a recombinant adenovirus through homologous recombination. Expression of the *Uch l1-* or β-*gal*-gene is achieved by removal of the stuffer sequence between the loxP sequences by Cre recombinase (expressed by co-transfection with pAx CANCre DNA).

Immunizing with different ubiquitin-carrier conjugates produced five antibodies and, among them, US-1 was found to be specifically reactive to mono-Ub (16). Immune complexes of US-1 and ^{125}I-mono-Ub were obtained by centrifuge and counted in a gamma counter. The inhibition for the tracer bound to the antibody in the presence of lysates was measured and mono-Ub level was determined from the standard curve generated by unlabeled Ub (16). Monoclonal antibody FK2 that recognizes conjugated-multi-ubiquitin chain was used for immunoassay (sandwich ELISA) for multi-ubiquitin chains as described (17,18). This ELISA system shows an only negligible reactivity to free-Ub (17).

Fractionation, immunoaffinity purification and immunoblotting

Mouse brains were homogenized in lysis buffer (50 mM NaH_2PO_4/300 mM NaCl/10 mM imidazole, containing a complete protease inhibitor cocktail, pH 8.0) and centrifuged at 70 000*g* for 1 h to yield a cytosolic fraction. The nuclear fraction was extracted with lysis buffer containing 10% NP-40 and 400 mM NaCl. Insoluble materials were dissolved with 8 M urea. For pull-down assays, 200 µg of His_6-tagged UCH $L1^{WT, C90S, D30K}$ and 40 µl of Ni-NTA Agarose (Qiagen) were added to 750 µl mouse brain lysate containing 6 mg total protein. After gentle rotation overnight at 4°C, the Ni-NTA beads were washed three times with 200 µl of wash buffer (50 mM NaH_2PO_4/300 mM NaCl/20 mM imidazole, pH 8.0). The beads were eluted with 3 × 40 µl elution buffer (50 mM NaH_2PO_4/300 mM NaCl/250 mM imidazole, pH 8.0) and subjected to SDS–PAGE, stained with Coomassie brilliant blue (CBB) or immunoblotted. Densitiometric analysises were done using software PD QUEST (BioRad). For TOF analysis, 1 µl samples were spotted onto H4 hydrophobic-coated Protein Chip Array (Ciphergen Biosystems, Palo Alto, CA, USA) after desalting with a C_{18} zip tip column. The ionized proteins were detected and accurate mass was determined based on TOF analysis. TOF mass spectra were collected in the positive ion mode and signal averages of 50 laser shots were used to generate each spectrum. After SDS–PAGE on a 10–20% gradient gel, protein bands migrating at ~8 kDa were excised and digested within the gel with trypsin (Sigma). Digested peptide samples were then introduced via nano-spray into a QSTAR Pulsar LC/MS/MS system (Applied Biosystems, Foster City, CA, USA). Immunoblotting was performed as described (10) using antibodies to Ub (1 : 100, Chemicon, MAB1510) and UCH L1 (1 : 1000, Chemicon, polyclonal). The Ub antibody MAB1510 is reactive to both free and conjugated forms of Ub in immunoblotting (15). The epitopes of UCH L1 antibody were confirmed to recognize the region encoded by other than exons 7 and 8 of *Uch l1* gene, by using UCH $L1^{gad}$ protein produced by *E. coli* expression system. Ub and $(Ub)_n$ were purchased from Boston Biochem, MA, USA.

Immunohistochemistry, immunofluorescence and electron microscopy

Twelve-week-old mouse brain and sciatic nerve sections were analyzed by immunocytochemistry as previously described (10) using antibodies to Ub that is predominantly reactive to free Ub in immuno-histochemistry (1 : 100, Sigma) and UCH-L1 (1 : 40, Medac; monoclonal). Antibodies to neurofilament-M (NF; 1 : 200, Chemicon, monoclonal), glial fibrillary acidic protein (GFAP; 1 : 200, Chemicon, monoclonal), proteolipid protein (PLP; 1 : 200, Chemicon, monoclonal) and myelin basic protein (MBP; 1 : 200, QED bioscience, monoclonal) were used as neuronal, astrocytes, oligodendrocytes, schwann cell markers, individually. For immunofluorescence studies, anti-mouse-Cy3 or -FITC or anti-rabbit-conjugated-Cy3 or -FITC (1 : 500, Jackson Immuno Research) were used as secondary antibodies. MEF cells and SH-SY5Y cells were analyzed by immunofluorescence using either anti-flag tag (1 : 200, Sigma) or anti-Ub (1 : 100, Sigma) as the primary antibodies. Ultrastrucal studies by electron microscopy were performed as described using sciatic nerve (11).

Quantitative RT–PCR analysis and dual luciferase assays

Primers for the mouse *Uch l3* and four ubiquitin genes were designed and comparative reverse transcription–PCR (RT–PCR) was performed using Taq Man probe with the ABI PRISM 7700 (Applied Biosystems) using total RNA from wild-type and *gad* mouse brain ($n = 3$). The dual luciferase assay was performed using the +18 to +1227 bp region of the human Ub C promoter generated from human genomic DNA as per the manufacturer's instructions (Promega).

Pulse chase analysis

Transfected MEF cells were washed and incubated with methionine-free medium for 1 h. The cells were then pulsed with 200 µCi/ml [^{35}S]-Met (NEN) for 1 h and then washed and chased with 30 mM methionine for 30 h. At 0, 2, 8, 20 and 30 h the cells were harvested for immunoprecipitation with anti-Ub. Following SDS–PAGE on a 15% gel, radioactive bands were detected using the image analysis software PD QUEST (BioRad).

Transgenic UCH L1 mouse

Flag tagged mouse UCH L1 was subcloned into pEF-Bos vector under the strong promoter EF-1α. This plasmid was linearized by digestion with *Hind*III/*Aat*II, gel-purified and extracted twice with phenol/chloroform. A 2 µg/ml solution of linearized plasmid was used for pronuclear microinjection. Offspring were screened for the presence of the transgene by PCR of tail DNA. Expression of transgenic *Uch l1* mRNA was confirmed by reverse transcription of total RNA (5 µg) and subsequent PCR using specific primers (Fig. 5A). Primers to β-actin were used for internal controls.

Molecular simulation

Mouse UCH L1 was automatically modeled using Modeler software with Insight (MSI) interface. Briefly, mouse UCH L1 was modeled after the data from the crystal structure of human UCH L3 using the ClustralW algorithm. Human UCH L3 was used to derive spatial restraints expressed as probability density functions (14). These functions are used to constrain C^{α}–C^{α} distances, main chain N–O distances, main chain and side chain dihedral angles, etc. The individual constraints were assembled

into a single molecular probability density function (MPDF). The three-dimensional protein model was then obtained by optimizing this MPDF. The optimization procedure itself employed a variable target function method with a conjugate gradient minimization scheme followed by an optional restrained simulated annealing molecular dynamics scheme.

Steady-state kinetics

Steady-state kinetic measurements were conducted at 25°C in assay buffer (50 mM HEPES pH 7.5, 0.5 mM EDTA, containing 0.1 mg/ml ovalbumin and 1 mM DTT). Concentrations of enzymes were 5 nM for UCH L1 and 5 mM for D30K- and C90S-UCH L1 mutants. Ubiquitin-7-amido-4-methylcoumarin (Ub-AMC; Boston Biochem, MA, USA) served as substrate at different concentrations, and AMC production was monitored continuously by fluorescence (Wallace 1420 multilabel counter, Perkin Elmer, Turk, Finland; $\lambda_{ex} = 355$ nm, $\lambda_{em} = 460$ nm). For competition/inhibition by ubiquitin, enzymes were pre-incubated with ubiquitin for 5 min at 25°C before adding substrates. Initial velocity data were used to determine values for K_m, K_i and k_{cat} from non-linear fits of the Michaelis–Menten equation with the program PRISM (GraphPad, San Diego, CA, USA).

ACKNOWLEDGEMENTS

We thank the following people for their contributions to this work: T. Kikuchi, T. Kokubo, R. Takahashi and Y. Imai for helpful discussions; S.-M. Tilghman for kind gift of *Uch l3*$^{\Delta 3\text{-}7}$ mouse; T. Kikuchi for technical assistance with tissue sections; A. Kanou for modeling (Ryoka Systems Inc.); K. Arimoto and J. Ando for TOF MASS analysis (Applied Biosystems); F. Melandri (Boston Biochem) for advice regarding steady-state kinetic measurements; S. Kohsaka for providing SH-SY5Y cells; and M. Shikama for the care and breeding of animals. This work was supported by grants-in-aid from the Ministry of Health, Labor and Welfare of Japan, grants-in-aid for scientific research from the Ministry of Education, Culture, Sports, Science and Technology of Japan, a grant from the Organization for Pharmaceutical Safety and Research, and a grant from Japan Science and Technology Cooperation. S.A. is a fellow of the Japan Society for the Promotion of Science (JSPS). Y.-L.W. is a fellow of the Japan Foundation for Aging and Health.

REFERENCES

1. Weissman, A.M. (2001) Themes and variations on ubiquitylation. *Nat. Rev. Mol. Cell. Biol.*, **2**, 169–178.
2. Tran, P.B. and Miller, R.J. (1999) Aggregates in neurodegenerative disease: crowds and power? *Trends Neurosci.*, **22**, 194–197.
3. Wilkinson, K.D., Laleli-Sahin, E., Urbauer, J., Larsen, C.N., Shih, G.H., Haas, A.L., Walsh, S.T. and Wand, A.J. (1999) The binding site for UCH-L3 on ubiquitin: mutagenesis and NMR studies on the complex between ubiquitin and UCH-L3. *J. Mol. Biol.*, **291**, 1067–1077.
4. Larsen, C.N., Krantz, B.A. and Wilkinson, K.D. (1998) Substrate specificity of deubiquitinating enzymes: ubiquitin C-terminal hydrolases. *Biochemistry*, **37**, 3358–3368.
5. Finley, D., Bartel, B. and Varshavsky, A. (1989) The tails of ubiquitin precursors are ribosomal proteins whose fusion to ubiquitin facilitates ribosome biogenesis. *Nature*, **338**, 394–401.
6. Wilkinson, K.D., Lee, K.M., Deshpande, S., Duerksen-Hughes, P., Boss, J.M. and Pohl, J. (1989) The neuron-specific protein PGP 9.5 is a ubiquitin carboxyl-terminal hydrolase. *Science*, **246**, 670–673.
7. Wilkinson, K.D., Deshpande, S. and Larsen, C.N. (1992) Comparisons of neuronal (PGP 9.5) and non-neuronal ubiquitin C-terminal hydrolases. *Biochem. Soc. Trans.*, **20**, 631–637.
8. Lowe, J., McDermott, H., Landon, M., Mayer, R.J. and Wilkinson, K.D. (1990) Ubiquitin carboxyl-terminal hydrolase (PGP 9.5) is selectively present in ubiquitinated inclusion bodies characteristic of human neurodegenerative diseases. *J. Pathol.*, **161**, 153–160.
9. Leroy, E., Boyer, R., Auburger, G., Leube, B., Ulm, G., Mezey, E., Harta, G., Brownstein, M.J., Jonnalagada, S., Chernova, T. *et al.* (1998) The ubiquitin pathway in Parkinson's disease. *Nature*, **395**, 451–452.
10. Saigoh, K., Wang, Y.L., Suh, J.G., Yamanishi, T., Sakai, Y., Kiyosawa, H., Harada, T., Ichihara, N., Wakana, S., Kikuchi, T. *et al.* (1999) Intragenic deletion in the gene encoding ubiquitin carboxy-terminal hydrolase in *gad* mice. *Nat. Genet.*, **23**, 47–51.
11. Kikuchi, T., Mukoyama, M., Yamazaki, K. and Moriya, H. (1990) Axonal degeneration of ascending sensory neurons in gracile axonal dystrophy mutant mouse. *Acta. Neuropathol. (Berl.)*, **80**, 145–151.
12. Wilkinson, K.D. (1997) Regulation of ubiquitin-dependent processes by deubiquitinating enzymes. *FASEB J.*, **11**, 1245–1256.
13. Liu, Y., Fallon, L., Lashuel, H.A., Liu, Z. and Lansbury, P.T. (2002) The UCH-L1 gene encodes two opposing enzymatic activities that affect alpha-synuclein degradation and Parkinson's disease susceptibility. *Cell*, **111**, 209–218.
14. Johnston, S.C., Larsen, C.N., Cook, W.J., Wilkinson, K.D. and Hill, C.P. (1997) Crystal structure of a deubiquitinating enzyme (human UCH-L3) at 1.8 Å resolution. *EMBO J.*, **16**, 3787–3796.
15. Morimoto, T., Ide, T., Ihara, Y., Tamura, A. and Kirino, T. (1996) Transient ischemia depletes free ubiquitin in the gerbil hippocampal CA1 neurons. *Am. J. Pathol.*, **148**, 249–257.
16. Takada, K., Hibi, N., Tsukada, Y., Shibasaki, T. and Ohkawa, K. (1996) Ability of ubiquitin radioimmunoassay to discriminate between mono-ubiquitin and multi-ubiquitin chains. *Biochim. Biophys. Acta*, **1290**, 282–288.
17. Fujimuro, M., Sawada, H. and Yokosawa, H. (1994) Production and characterization of monoclonal antibodies specific to multi-ubiquitin chains of polyubiquitinated proteins. *FEBS Lett.*, **349**, 173–180.
18. Takada, K., Nasu, H., Hibi, N., Tsukada, Y., Ohkawa, K., Fujimuro, M., Sawada, H. and Yokosawa, H. (1995) Immunoassay for the quantification of intracellular multi-ubiquitin chains. *Eur. J. Biochem.*, **233**, 42– 47.
19. Swaminathan, S., Amerik, A.Y. and Hochstrasser, M. (1999) The Doa4 deubiquitinating enzyme is required for ubiquitin homeostasis in yeast. *Mol. Biol. Cell*, **10**, 2583–2594.
20. Amerik, A.Y., Nowak, J., Swaminathan, S. and Hochstrasser, M. (2000) The Doa4 deubiquitinating enzyme is functionally linked to the vacuolar protein-sorting and endocytic pathways. *Mol. Biol. Cell*, **11**, 3365–3380.
21. Johnston, S.C., Riddle, S.M., Cohen, R.E. and Hill, C.P. (1999) Structural basis for the specificity of ubiquitin C-terminal hydrolases. *EMBO J.*, **18**, 3877–3887.
22. Shih, S.C., Sloper-Mould, K.E. and Hicke, L. (2000) Monoubiquitin carries a novel internalization signal that is appended to activated receptors. *EMBO J.*, **19**, 187–198.
23. Nakatsu, F., Sakuma, M., Matsuo, Y., Arase, H., Yamasaki, S., Nakamura, N., Saito, T. and Ohno, H. (2000) A di-leucine signal in the ubiquitin moiety. Possible involvement in ubiquitination-mediated endocytosis. *J. Biol. Chem.*, **275**, 26213–26219.
24. Bennett, M.C., Bishop, J.F., Leng, Y., Chock, P.B., Chase, T.N. and Mouradian, M.M. (1999) Degradation of alpha-synuclein by proteasome. *J. Biol. Chem.*, **274**, 33855–33858.
25. Rochet, J.C. and Lansbury, P.T. Jr (2000) Amyloid fibrillogenesis: themes and variations. *Curr. Opin. Struct. Biol.*, **10**, 60–68.
26. Shimura, H., Hattori, N., Kubo, S., Mizuno, Y., Asakawa, S., Minoshima, S., Shimizu, N., Iwai, K., Chiba, T., Tanaka, K. *et al.* (2000) Familial Parkinson disease gene product, parkin, is a ubiquitin-protein ligase. *Nat. Genet.*, **25**, 302–305.
27. Imai, Y., Soda, M., Inoue, H., Hattori, N., Mizuno, Y. and Takahashi, R. (2001) An unfolded putative transmembrane polypeptide, which can lead to endoplasmic reticulum stress, is a substrate of Parkin. *Cell*, **105**, 891–902.

28. Bizzi, A., Schaetzle, B., Patton, A., Gambetti, P. and Autilio-Gambetti, L. (1991) Axonal transport of two major components of the ubiquitin system: free ubiquitin and ubiquitin carboxyl-terminal hydrolase PGP 9.5. *Brain Res.*, **548**, 292–299.
29. Momose, Y., Murata, M., Kobayashi, K., Tachikawa, M., Nakabayashi, Y., Kanazawa, I. and Toda, T. (2002) Association studies of multiple candidate genes for Parkinson's disease using single nucleotide polymorphisms. *Ann. Neurol.*, **51**, 133–136.
30. Satoh, J. and Kuroda, Y. (2001) A polymorphic variation of serine to tyrosine at codon 18 in the ubiquitin C-terminal hydrolase-L1 gene is associated with a reduced risk of sporadic Parkinson's disease in a Japanese population. *J. Neurol. Sci.*, **189**, 113–117.
31. Wang, J., Zhao, C.Y., Si, Y.M., Liu, Z.L., Chen, B. and Yu, L. (2002) ACT and UCH-L1 polymorphisms in Parkinson's disease and age of onset. *Mov. Disord.*, **17**, 767–771.
32. Maraganore, D.M., Farrer, M.J., Hardy, J.A., Lincoln, S.J., McDonnell, S.K. and Rocca, W.A. (1999) Case-control study of the ubiquitin carboxy-terminal hydrolase L1 gene in Parkinson's disease. *Neurology*, **53**, 1858–1860.
33. Polymeropoulos, M.H., Lavedan, C., Leroy, E., Ide, S.E., Dehejia, A., Dutra, A., Pike, B., Root, H., Rubenstein, J., Boyer, R. *et al.* (1997) Mutation in the alpha-synuclein gene identified in families with Parkinson's disease. *Science*, **276**, 2045–2047.
34. Kitada, T., Asakawa, S., Hattori, N., Matsumine, H., Yamamura, Y., Minoshima, S., Yokochi, M., Mizuno, Y. and Shimizu, N. (1998) Mutations in the parkin gene cause autosomal recessive juvenile parkinsonism. *Nature*, **392**, 605–608.
35. Bonifati, V., Rizzu, P., Van Baren, M.J., Schaap, O., Breedveld, G.J., Krieger, E., Dekker, M.C., Squitieri, F., Ibanez, P., Joosse, M. *et al.* (2002) Mutations in the DJ-1 gene associated with autosomal recessive early-onset Parkinsonism. *Science.* Published online 21 November 2002; 10.1126/science.1077209.
36. Shimura, H., Schlossmacher, M.G., Hattori, N., Frosch, M.P., Trockenbacher, A., Schneider, R., Mizuno, Y., Kosik, K.S. and Selkoe, D.J. (2001) Ubiquitination of a new form of alpha-synuclein by parkin from human brain: implications for Parkinson's disease. *Science*, **293**, 263–269.
37. Abeliovich, A., Schmitz, Y., Farinas, I., Choi-Lundberg, D., Ho, W.H., Castillo, P.E., Shinsky, N., Verdugo, J.M., Armanini, M., Ryan, A. *et al.* (2000) Mice lacking alpha-synuclein display functional deficits in the nigrostriatal dopamine system. *Neuron*, **25**, 239–252.
38. Kurihara, L.J., Semenova, E., Levorse, J.M. and Tilghman, S.M. (2000) Expression and functional analysis of Uch-L3 during mouse development. *Mol. Cell. Biol.*, **20**, 2498–2504.

American Journal of Pathology, Vol. 165, No. 4, October 2004

Cell Injury, Repair, Aging and Apoptosis

Two Closely Related Ubiquitin C-Terminal Hydrolase Isozymes Function as Reciprocal Modulators of Germ Cell Apoptosis in Cryptorchid Testis

Jungkee Kwon,*† Yu-Lai Wang,* Rieko Setsuie,*‡ Satoshi Sekiguchi,† Yae Sato,*‡ Mikako Sakurai,*‡ Mami Noda,‡ Shunsuke Aoki,* Yasuhiro Yoshikawa,† and Keiji Wada*

From the Department of Degenerative Neurological Diseases, National Institute of Neuroscience, National Center of Neurology and Psychiatry, Kodaira, Tokyo; the Department of Biomedical Science,† Graduate School of Agricultural and Life Sciences, University of Tokyo, Tokyo; and the Laboratory of Pathophysiology,‡ Graduate School of Pharmaceutical Sciences, Kyushu University, Fukuoka, Japan*

The experimentally induced cryptorchid mouse model is useful for elucidating the *in vivo* molecular mechanism of germ cell apoptosis. Apoptosis, in general, is thought to be partly regulated by the ubiquitin-proteasome system. Here, we analyzed the function of two closely related members of the ubiquitin C-terminal hydrolase (UCH) family in testicular germ cell apoptosis experimentally induced by cryptorchidism. The two enzymes, UCH-L1 and UCH-L3, deubiquitinate ubiquitin-protein conjugates and control the cellular balance of ubiquitin. The testes of gracile axonal dystrophy (*gad*) mice, which lack UCH-L1, were resistant to cryptorchid stress-related injury and had reduced ubiquitin levels. The level of both anti-apoptotic (Bcl-2 family and XIAP) and prosurvival (pCREB and BDNF) proteins was significantly higher in *gad* mice after cryptorchid stress. In contrast, *Uchl3* knockout mice showed profound testicular atrophy and apoptotic germ cell loss after cryptorchid injury. Ubiquitin level was not significantly different between wild-type and *Uchl3* knockout mice, whereas the levels of Nedd8 and the apoptotic proteins p53, Bax, and caspase3 were elevated in *Uchl3* knockout mice. These results demonstrate that UCH-L1 and UCH-L3 function differentially to regulate the cellular levels of anti-apoptotic, prosurvival, and apoptotic proteins during testicular germ cell apoptosis. *(Am J Pathol 2004, 165:1367–1374)*

In the ubiquitin-proteasome system, the levels of poly- and monoubiquitin are strictly controlled by the balance of two groups of specific enzymes: ubiquitinating enzymes (E1, E2, and E3) and deubiquitinating enzymes (DUBs).[1,2] DUBs are subdivided into ubiquitin C-terminal hydrolases (UCHs) and ubiquitin-specific proteases (UBPs).[3,4] The genes for at least four UCHs, UCH-L1 and UCH-L3, UCH-L4, and UCH-L5, have been identified in mice.[5,6] Among them, UCH-L1 and UCH-L3 predominate; these isozymes have 52% amino acid identity and share significant structural similarity;[7] however, the distribution of these two isozymes is quite distinct in that UCH-L3 mRNA is expressed ubiquitously whereas UCH-L1 mRNA is selectively expressed in the testis/ovary and neuronal cells.[7–10] Despite the high-sequence homology, the *in vitro* hydrolytic activities of these two enzymes differ significantly. The activity (Kcat) of UCH-L3 is more than 200-fold higher than UCH-L1 when a fluorogenic ubiquitin substrate is used.[11] In addition to its relatively weak hydrolase activity, UCH-L1 exhibits dimerization-dependent ubiquityl ligase activity.[11] In contrast, UCH-L3 has little or no ligase activity compared with UCH-L1.[11] It was recently suggested that UCH-L1 has anti-proliferative activity in tumor cells, and that its expression is induced in response to tumor growth.[12] Furthermore, UCH-L1 associates with monoubiquitin and prolongs ubiquitin half-life in neurons.[13] Other work demonstrated that UCH-L3 binds to Nedd8 and subsequently processes its C-terminus.[14] Nedd8 is a small ubiquitin-like protein that shares with ubiquitin the ability to be conjugated to a lysine residue in a substrate protein.[15] Covalent conjugation of proteins by Nedd8 is an important form of the posttranscriptional modification and plays a critical role in many cellular processes.[16] These conju-

Supported by Grants-in-Aid for Scientific Research from the Ministry of Health, Labor, and Welfare of Japan; Grants-in-Aid for Scientific Research from the Ministry of Education, Culture, Sports, Science, and Technology of Japan; a grant from Pharmaceuticals and Medical Devices Agency of Japan; and a grant from Japan Science and Technology Agency.

Accepted for publication June 24, 2004.

Address reprint requests to Keiji Wada, Department of Degenerative Neurological Disease, National Institute of Neuroscience, National Center of Neurology and Psychiatry, Kodaira, Tokyo, 187-8502, Japan. E-mail: wada@ncnp.go.jp.

gates are regulated by a large number of deconjugating enzymes. This activity is unique to UCH-L3 because UCH-L1 is relatively weak to cleave the C terminus of Nedd8.[14–16] Collectively, these data suggest that the two mouse isozymes, UCH-L1 and UCH-L3, have distinct but overlapping functions. In addition, we recently found that *gad* mice, which lack UCH-L1 expression, show reduced retinal cell apoptosis in response to ischemia, suggesting that UCH-L1 may promote apoptosis.[17]

Our previous work focused on the possibility that UCH-L1 and UCH-L3 exhibit functional diversity during spermatogenesis. We showed that both UCH-L1 and UCH-L3 are strongly but reciprocally expressed in the testis during spermatogenesis,[18] suggesting that each isozyme may have a distinct function in the testis. To elucidate the pathophysiological roles of these two isozymes in the testis, our present work examines the extent of heat-induced stress using experimentally induced cryptorchidism in *Uchl3* knockout[7] and *gad* mice.[8] Normally, the testes are maintained in the scrotum at a temperature lower than that of the abdomen. Exposure of a testis to higher body temperature via experimentally induced cryptorchidism results in rapid degeneration of testicular germ cells.[19–22] Recent studies show that testicular germ cell degeneration in cryptorchid testes occurs via apoptosis, and that protein and lipid oxidation, along with p53 promote germ cell death.[23–25] The ubiquitin-proteasome system is required for the subsequent degradation of the damaged testicular germ cells.[26–28] Here, we show that both UCH-L1 and UCH-L3 have reciprocal functions in testicular germ cells during cryptorchid-induced apoptosis. Our data show that the absence of UCH-L1 causes resistance to cryptorchid-induced testicular germ cell apoptosis, and that the knockout of UCH-L3 promotes germ cell apoptosis after cryptorchid injury.

Materials and Methods

Animals

We used 8-week-old *Uchl3* knockout (C57BL/6J)[7,18] and *gad*[8,18,29] (CBA/RFM) male mice. *Uchl3* knockout mice were generated by the standard method using homologously recombinant ES cells, and the knockout line was back-crossed several times to C57BL/6J mice.[7] The *gad* mouse is an autosomal recessive mutant that was obtained by crossing CBA and RFM mice.[8] The *gad* line was maintained by intercrossing for more than 20 generations.[8,29] Both strains were maintained at our institute. Animal care and handling were in accordance with institutional regulations for animal care and were approved by the Animal Investigation Committee of the National Institute of Neuroscience, National Center of Neurology and Psychiatry, Tokyo, Japan.

Unilateral Experimental Cryptorchidism

Unilateral cryptorchidism was experimentally induced under pentobarbital anesthesia (Abbott Laboratories, North Chicago, IL).[20,22] Briefly, a midline abdominal incision was made, and the left testis was displaced from scrotum and fixed to the upper abdominal wall. The right testis remained in the scrotum as an intact control within the same animal. At 0, 4, 7, and 14 days after the operation, four control and four cryptorchid testes were harvested to determine testis weight.

Histological and Immunohistochemical Assessment of Testes

Testes were embedded in paraffin wax after fixation in 4% paraformaldehyde, sectioned at 4-μm thickness, and stained with hematoxylin and eosin.[29] Light microscopy was used for routine observations. For immunohistochemical staining, the sections were incubated with 10% goat serum for 1 hour at room temperature, followed by incubation overnight at 4°C with a rabbit polyclonal antibody against ubiquitin (1:500; DakoCytomation, Glostrup, Denmark) or Nedd8 (1:500; Alexis Biochemicals, San Diego, CA) diluted in phosphate-buffered saline (PBS) containing 1% bovine serum albumin. Sections were then incubated with fluorescein isothiocyanate-conjugated goat anti-rabbit IgG (1:200; Jackson ImmunoResearch, West Grove, PA) for 1 hour at room temperature and examined by confocal laser-scanning microscopy (Olympus, Tokyo, Japan).

Apoptotic cells in testicular tissues were identified by terminal deoxynucleotidyl transferase (TdT)-mediated nick-end labeling (TUNEL) using the DeadEnd Fluorimetric TUNEL system kit (Promega, Madison, WI) and the anti-PARP p85 fragment pAb (Promega) according to the manufacturer's instructions.

Quantitative Analysis of Apoptotic Germ Cells

The number of apoptotic cells was determined by counting the positively stained nuclei in 30 circular seminiferous tubule cross-sections per testis section.[23,29] The proportion of seminiferous tubules containing apoptotic germ cells was calculated by dividing the number of seminiferous tubules containing apoptotic cells by the total number of seminiferous tubules. The incidence of apoptotic cells per apoptotic cell-containing seminiferous tubule was categorized into three groups, defined as 1 to 5, 6 to 10, and >11 positive cells.

Western Blotting

Western blots were performed as previously reported.[8,18,29] Total protein (5 μg/lane) was subjected to sodium dodecyl sulfate-polyacrylamide gel electrophoresis using 15% gels (Perfect NT Gel; DRC, Japan). Proteins were electrophoretically transferred to polyvinylidene difluoride membranes (Bio-Rad, Hercules, CA) and blocked with 5% nonfat milk in TBS-T [50 mmol/L Tris base, pH 7.5, 150 mmol/L NaCl, 0.1% (w/v) Tween-20]. The membranes were incubated individually with one or more primary antibodies to UCH-L1 and UCH-L3 (1:1000; peptide antibodies[18]), Bcl-2, Bcl-xL, Bax, p53, and caspase-3, (1:1000; all from Cell Signaling Technology, Beverly, MA), phosphorylated cyclic AMP response element-binding protein (pCREB, 1:500; Upstate Biotech-

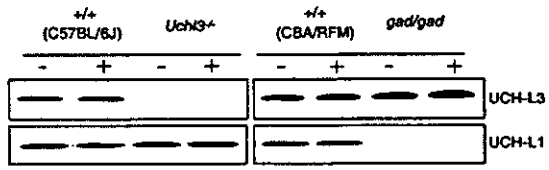

Figure 1. Western blotting analyses of both UCH-L3 and UCH-L1 in the testes of *gad* and *Uchl3* knockout mice, respectively, on day 4 after cryptorchid injury. Scrotal and cryptorchid testes did not differ significantly with respect to protein expression (−, scrotal testes; +, cryptorchid testes).

nology, Waltham, MA), brain-derived neurotrophic factor (BDNF, 1:500; Santa Cruz Biotechnology, Santa Cruz, CA), XIAP (1:500; Transduction Laboratories, Franklin Lakes, NJ), polyubiquitin (1:1000, clone FK-2; Medical & Biological Laboratories, Nagoya, Japan), monoubiquitin (1:1000, u5379; Sigma-Aldrich, St. Louis, MO), and Nedd8 (1:1000; Alexis Biochemicals, San Diego, CA). Blots were further incubated with peroxidase-conjugated goat anti-mouse IgG or goat anti-rabbit IgG (1:5000; Pierce, Rockford, IL) for 1 hour at room temperature. Immunoreactions were visualized using the SuperSignal West Dura extended duration substrate (Pierce) and analyzed with a Chemi-Imager (Alpha Innotech, San Leandro, CA). Each protein level was relatively quantificated after analysis with a ChemiImager using AlphaEase software.

Statistical Analysis

The mean and SD were calculated for all data (presented as mean ± SD). One-way analysis of variance was used for all statistical analyses.

Results

Level of Two UCH Isozymes in Scrotal and Cryptorchid Testes from Uchl3 Knockout and Gad Mice

We first confirmed the lack of UCH-L3 protein in the testes from *Uchl3* knockout mice by Western blotting (Figure 1). Similarly, we did not detect UCH-L1 protein in the testes of *gad* mice (Figure 1), as we previously observed.[13] Thus, in a biochemical sense, *gad* mice are analogous to *Uchl1*-null mice.[8,13] Compensatory level of UCH-L3 and UCH-L1 in *gad* and *Uchl3* knockout mice, respectively, was not observed (Figure 1; compare UCH-L3/UCH-L1 level with that of wild-type control mice). Experimental cryptorchidism did not affect UCH-L3 level in *gad* or wild-type control mice. Similarly, cryptorchidism did not affect UCH-L1 level in *Uchl3* knockout and wild-type control mice (Figure 1). Quantitative reverse transcriptase-polymerase chain reaction analysis showed that transcription from the *Uchl3* and *Uchl1* in both scrotal and cryptorchid testes from *gad* and *Uchl3* knockout mice was not significantly different from that measured in the corresponding wild-type control mice (data not shown). These results suggest that the level of UCH-L3 is regulated independently of UCH-L1 in the mouse testis, and that cryptorchid injury does not affect the level of either protein.

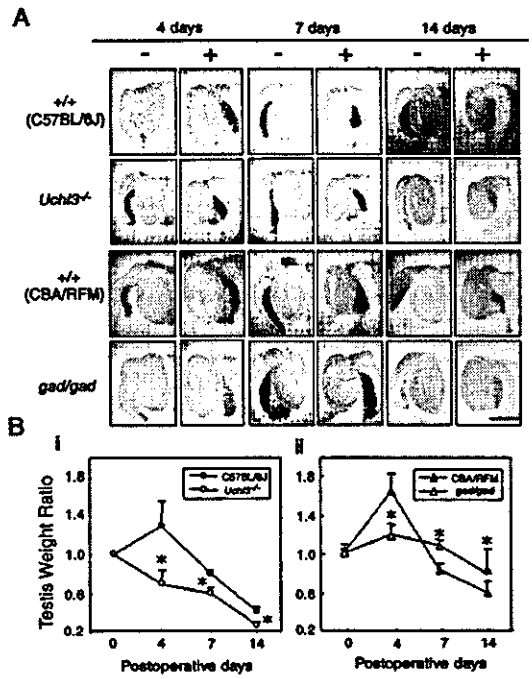

Figure 2. Comparison of testicular sizes and weights after experimental cryptorchidism. **A:** Gross images of changes in testicular size throughout time in two wild-type (C57BL/6J and CBA/RFM), *Uchl3* knockout, and *gad* mice (−, scrotal testes; +, cryptorchid testes). **B:** Ratio of cryptorchid to scrotal testis weight on days 0, 4, 7, and 14 after injury. i: Throughout time, the ratio for *Uchl3* knockout mice (**open circles**) differed significantly compared with wild-type mice (**filled circles**). ii: The ratio for *gad* mice (**open triangles**) did not differ significantly throughout time compared with wild-type mice (**closed triangles**). ($n = 4$; *, $P < 0.05$). Scale bar, 5 mm. Original magnifications, ×40.

Changes in Testicular Weight and Structure in Cryptorchid Uchl3 Knockout and Gad Mice

Unilateral cryptorchidism was surgically induced in *Uchl3* knockout and *gad* mice, and testes were evaluated on days 0, 4, 7, and 14 after the operation (Figure 2). Nonoperated (scrotal) testes served as controls for the evaluation of testicular weight and histochemistry. Cryptorchid testes from *Uchl3* knockout mice appeared smaller than the nonoperated controls at each time point, whereas the size of the cryptorchid testes from *gad* mice was similar to the controls (Figure 2A). Figure 2B shows the time course of the ratio of testicular weight of cryptorchid testes to scrotal testes. In wild-type mice (C57BL/6J and CBA/RFM), the ratio transiently increased 4 days after cryptorchid injury, most likely a consequence of inflammation-induced fluid accumulation[22,23] and biochemical changes observed. The ratio for these mice subsequently decreased below 1.0 by day 7. The ratio remained ~1.0 in *gad* mice (range,1.15 ~ 0.85), whereas it decreased significantly in *Uchl3* knockout mice compared with wild-type mice (Figure 2B). These results demonstrate that testes from *Uchl3* knockout and *gad* mice differ in their response to experimental cryptorchidism.

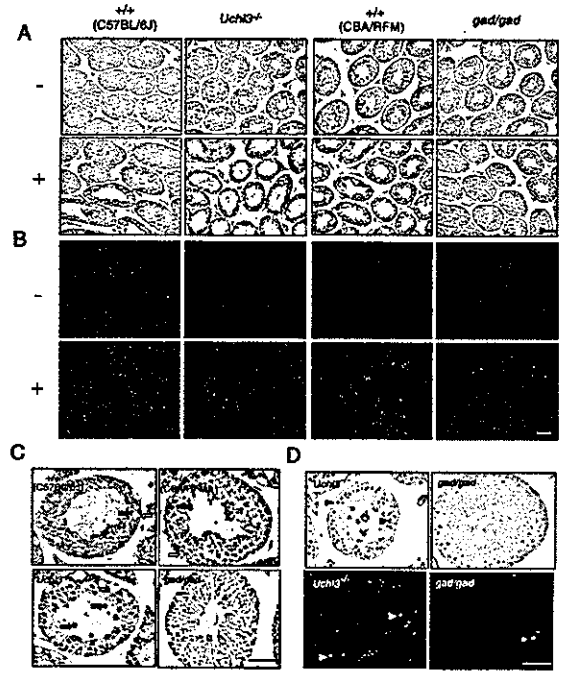

Figure 3. Histology and TUNEL staining of testicular cross sections after experimental cryptorchidism. **A:** Morphological analysis of seminiferous tubules on day 7 after cryptorchid injury. Note the germ cell loss and atrophy in cryptorchid testes compared with uninjured controls. (−, scrotal testes; +, cryptorchid testes). **B:** TUNEL staining of testicular cross-sections on day 7 after cryptorchid injury. Green fluorescence, TUNEL-positive cells; red fluorescence, nuclei stained with propidium iodide. **C:** Magnified cryptorchid testes sections. Pyknotic bodies (**filled arrows**) and Sertoli cell vacuolization (**open arrows**) were evident in cryptorchid testes of *Uchl3* knockout and the two wild-type (C57BL/6J and CBA/RFM) mice on day 7 after injury. **D:** PARP analysis to detect apoptotic germ cells in cryptorchid testes of *Uchl3* knockout and *gad* mice on day 7 after injury. The detection of apoptotic germ cells (**arrowheads, top**) by PARP analysis was consistent with that of apoptotic germ cells (**arrowheads, bottom**) by TUNEL analysis. Scale bar, 50 μm. Original magnifications: **A** and **B** ×100; **C** and **D** ×200.

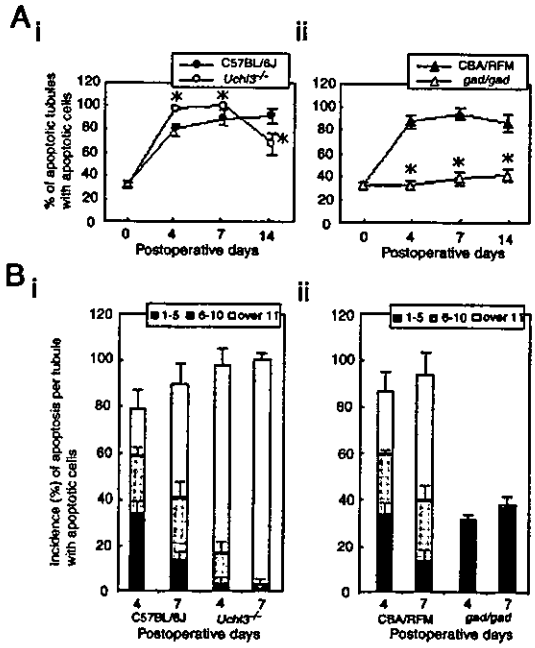

Figure 4. Quantitation of testicular germ cell apoptosis in testes after experimental cryptorchidism. **A:** The percentage of seminiferous tubules containing apoptotic germ cells in cryptorchid testes on days 0, 4, 7, and 14 after injury. **i:** The increase in the percentage of tubules containing apoptotic cells in the cryptorchid testes of *Uchl3* knockout mice is statistically significant compared with wild-type mice on days 4, 7, and 14. Each value represents the mean ± SD; *, $P < 0.05$. **ii:** The percentage of apoptotic tubules in cryptorchid testes of *gad* mice is significantly different on days 4, 7, and 14 after injury. Each value represents the mean ± SD; *, $P < 0.01$. **B:** Incidence of apoptosis per seminiferous tubule with apoptotic germ cells on days 4 and 7 after injury. The incidence of seminiferous tubules containing >11 apoptotic germ cells is significantly increased ($P < 0.05$) in cryptorchid testes of *Uchl3* knockout mice compared with wild-type mice. **i:** Comparison with *Uchl3* knockout mice. **ii:** Comparison with *gad* mice. Each value represents the mean ± SD.

Testicular Germ Cell Apoptosis in Cryptorchid Uchl3 Knockout and Gad Mice

To explore the mechanism underlying the observed differences between *Uchl3* knockout and *gad* cryptorchid testes, we prepared histological cross-sections on day 7 after testicular injury (Figure 3, A and C). The presence of nuclear pyknosis, multinucleated giant cells, and Sertoli cell vacuolization with germ cell loss in the germinal epithelium is indicative of cryptorchid testes.[22,23] These hallmarks of testicular injury were the most remarkable characteristics of cryptorchid testes from *Uchl3* knockout mice, demonstrating profound testicular atrophy and germ cell loss compared with wild-type mice (Figure 3, A and C). In contrast, no nuclear pyknosis, cellular shrinkage, or germ cell loss was observed in cryptorchid testes from *gad* mice. Spermatocytes and early spermatids comprised the majority of affected cell types in cryptorchid testes (Figure 3, A and C).

Germ cell apoptosis was further examined by TUNEL and PARP assays in tissue sections from postoperative day 7 mice (Figure 3, B and D). All but the *gad* cryptorchid testes showed a time-dependent increase in germ cell apoptosis during experimental cryptorchidism; germ cell apoptosis was always found in tubules that had germ cell loss on days 4, 7, and 14 (Figure 3, B and D, and Figure 4). Compared to wild-type mice, the cryptorchid testes of *Uchl3* knockout mice showed a marked increase in apoptotic germ cells in response to testicular injury, whereas *gad* mice lacked cryptorchid-induced germ cell apoptosis (Figure 3B and Figure 4). By postoperative days 4 and 7, the percentage of seminiferous tubules containing apoptotic germ cells increased with statistical significance ($n = 4$) ($P < 0.05$) in cryptorchid testes of *Uchl3* knockout mice as compared with wild-type mice (Figure 4A). In addition, cryptorchid testes of *Uchl3* knockout mice showed a high incidence of seminiferous tubules containing >11 apoptotic germ cells on days 4 and 7 days as compared with wild-type mice (Figure 4B); however, germ cell apoptosis did not increase in cryptorchid testes of *gad* mice during postoperative days 4 to 14 ($P < 0.01$) (Figure 4, A and B).

Cellular Mono- and Polyubiquitin Level in Cryptorchid Uchl3 Knockout and Gad Mice

Ubiquitin is required for energy-dependent degradation of structurally altered proteins.[26] We previously reported that UCH-L1 binds ubiquitin and stabilizes ubiquitin turnover in neurons, and that the level of monoubiquitin is decreased in *gad* mice.[13] In a model of ischemic insult in the retina, ubiquitin induction was unexpectedly lower and ischemic

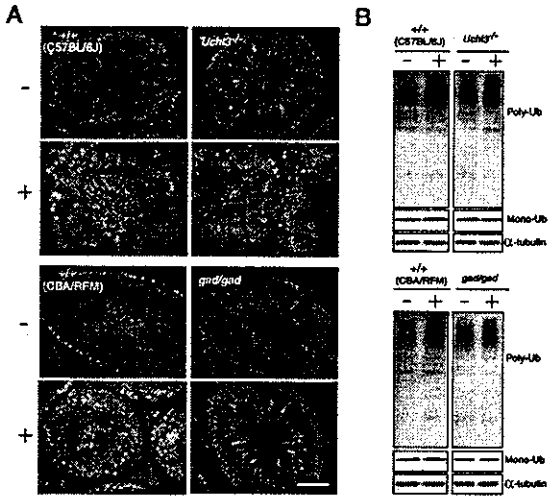

Figure 5. Immunohistochemical and Western blotting analyses of mono- and polyubiquitin in testes on day 7 after experimental cryptorchidism. **A:** Ubiquitin induction was not different between cryptorchid testes from *Uchl3* knockout and wild-type mice, whereas cryptorchid-induced ubiquitin induction in *gad* mice was reduced. Green fluorescence, ubiquitin-positive cells; red fluorescence, nuclei stained with propidium iodide. **B:** Polyubiquitin level in *Uchl3* knockout mice and the two wild-type (C57BL/6J and CBA/RFM) mice substantially increased after injury, whereas that in *gad* mice did not change significantly. Monoubiquitin level did not change after injury. Representative images from four independent experiments are shown (−, scrotal testes; +, cryptorchid testes). Scale bar, 50 μm. Original magnifications, ×200.

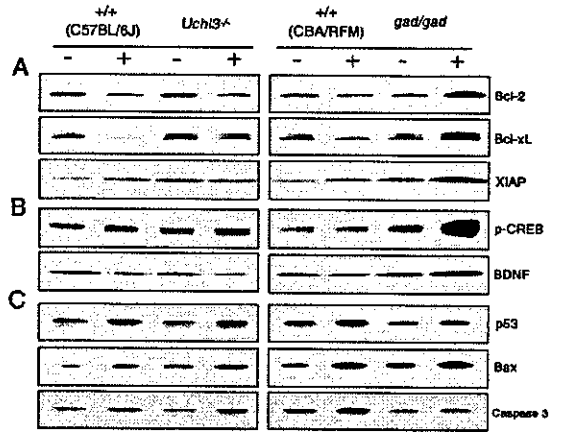

Figure 6. Western blotting analysis of anti-apoptotic, prosurvival, and apoptotic proteins in testes after experimental cryptorchidism. Total protein (5 μg per lane) was prepared from scrotal and cryptorchid testes on day 4 after cryptorchid injury. The expression levels of anti-apoptotic (**A**), prosurvival (**B**), and apoptotic (**C**) proteins in the cryptorchid testes of *Uchl3* knockout, *gad*, and the two wild-type (C57BL/6J and CBA/RFM) mice were significantly different compared with control mice. Representative images from four independent experiments are shown (−, scrotal testes; +, cryptorchid testes).

damage was weaker in the retina of *gad* mice (compared with wild-type mice) after ischemic insult.[17] To determine whether the increase in germ cell apoptosis in cryptorchid testes is associated with ubiquitin induction, we performed immunohistochemical analysis of testes from postoperative day 7 mice. Ubiquitin immunoreactivity increased substantially in cryptorchid testes from *Uchl3* knockout mice and the two wild-type mice, whereas those from *gad* mice showed only minor ubiquitin induction (Figure 5A). The scrotal testes of *Uchl3* knockout and *gad* mice did not show significant differences in ubiquitin induction compared with corresponding controls (Figure 5A). Interestingly, most of the increased ubiquitin induction was detected in spermatocytes and spermatids, consistent with the data on germ cell apoptosis after cryptorchid injury (Figure 3D and Figure 5A). Cryptorchid-induced polyubiquitin levels in the testes from *Uchl3* knockout and the two wild-type mice also increased substantially after injury, whereas the cryptorchid testes of *gad* mice showed no significant difference compared with scrotal testes (Figure 5B); however, the expression levels of monoubiquitin did not change significantly in any of the mice after cryptorchid injury.

Level of Anti-Apoptotic and Apoptotic Proteins in Cryptorchid Uchl3 Knockout and Gad Mice

We previously showed that anti-apoptotic proteins such as Bcl-2 and prosurvival proteins including phosphorylated cyclic AMP response element-binding protein (pCREB) are up-regulated in degenerated retina of *gad* mice.[17] These proteins are degraded by ubiquitination-mediated proteolysis.[30] We examined the expression of the Bcl-2 family proteins, XIAP, pCREB, and caspases to determine their role in testicular germ cell apoptosis after experimental cryptorchidism 4 days after injury in *Uchl3* knockout and *gad* mice. The level of anti-apoptotic proteins such as Bcl-2, Bcl-xL, and XIAP was up-regulated (323.8 ± 57.5, 262.3 ± 22.1, and 209.9 ± 11.7, respectively, as compared with wild type, 100) in the cryptorchid testes of *gad* mice compared with wild-type mice (Figure 6A). Additionally, pCREB, which is normally degraded in a ubiquitination-mediated manner,[30] was apparently highly up-regulated (259.0 ± 22.6, as compared with wild type, 100) in the cryptorchid testes of *gad* mice (Figure 6B). It has been demonstrated that pCREB activates genes that up-regulate trophic factors including BDNF.[31,32] Consistent with pCREB up-regulation, BDNF level also increased (203.0 ± 19.6, as compared with wild type, 100) in cryptorchid testes of *gad* mice (Figure 6B). Level was variable for anti-apoptotic, prosurvival, and apoptotic proteins in the cryptorchid testes of *Uchl3* knockout mice. The level of pCREB, p53, Bax, and caspase3 was slightly increased (169.9 ± 15.2, 152.6 ± 12.9, and 157.3 ± 14.0, respectively, as compared with scrotal testes, 100) in cryptorchid testes of *Uchl3* knockout mice compared with scrotal testes (Figure 6, B and C). Wild-type control mice had a similar expression level pattern except for pCREB. Because p53 acts as an upstream activator of Bax expression,[33] the observed Bax up-regulation after cryptorchid injury was consistent with the elevated p53 level in *Uchl3* knockout and wild-type control mice (Figure 6C). In contrast, BDNF was down-regulated (74.3 ± 7.7 as compared with wild type, 100) in cryptorchid testes of *Uchl3* knockout mice (Figure 6B). The down-regulation of BDNF combined with the up-regulation of pCREB suggests that BDNF might be regulated by another pathway that involves UCH-L3 but not pCREB.[34] Compared with scrotal testes, the expression of anti-apoptotic proteins decreased or was unchanged in cryptorchid testes of *Uchl3* knockout mice (Figure 6A).

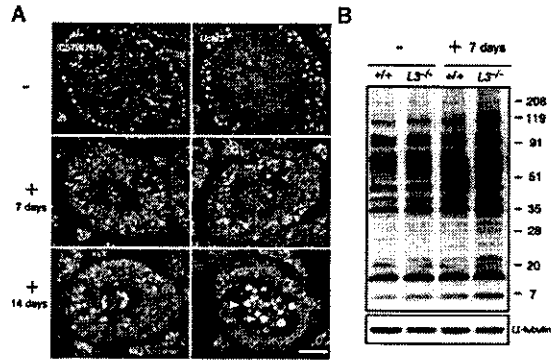

Figure 7. Immunohistochemical and Western blotting analyses of Nedd8 in testes from *Uchl3* knockout mice on days 7 and 14 after experimental cryptorchidism. **A:** Nedd8 induction in *Uchl3* knockout mice increased in both scrotal and cryptorchid testes. The shedding germ cells (**arrowheads**) in the cryptorchid testes of *Uchl3* knockout mice showed strong Nedd8 induction (−, scrotal testes; +7 days and + 4 days, cryptorchid testes). Green fluorescence, Nedd8-positive cells; red fluorescence, nuclei stained with propidium iodide. **B:** On day 7, the expression levels of Nedd8-conjugated proteins in *Uchl3* knockout mice were higher than in wild-type mice. Representative images of four independent experiments are shown. Scale bar, 50 μm. Original magnifications, ×200.

Nedd8 Level in Cryptorchid Uchl3 Knockout Mice

The varied expression levels of ubiquitin, anti-apoptotic, and apoptotic proteins in cryptorchid testes did not adequately explain the relatively exacerbated testicular atrophy and germ cell loss in *Uchl3* knockout mice compared with wild-type mice. We explored the underlying mechanism of this observation using the fact that UCH-L3 cleaves Nedd8.[14,16] We tested whether any change in Nedd8 expression correlated with greater testicular atrophy and germ cell loss in *Uchl3* knockout mice. Nedd8 immunoreactivity was highly detected in scrotal and cryptorchid testes from *Uchl3* knockout mice compared with wild-type mice (Figure 7A). The increased Nedd8 induction was mainly observed in spermatocytes and spermatids, and its expression pattern was similar to that of UCH-L3 during spermatogenesis.[18] These results suggest that Nedd8 may interact closely with UCH-L3 during testicular atrophy and germ cell loss. The cryptorchid testes of *Uchl3* knockout mice showed time-dependent and rapid Nedd8 induction compared with wild-type mice throughout the period 7 to 14 days after injury (Figure 7A). Moreover, the cryptorchid testes of *Uchl3* knockout mice showed strong Nedd8 induction in luminal shedding germ cells on day 14. An immunoblot of scrotal and cryptorchid testes proteins on day 7 confirmed the higher expression levels of Nedd8-conjugated proteins in *Uchl3* knockout mice as compared with wild-type mice (Figure 7B).

Discussion

During spermatogenesis, apoptosis controls germ cell numbers and eliminates defective germ cells to facilitate testicular homeostasis.[35–37] Recent studies indicate that ubiquitination targets proteins for degradation and modulates the turnover of various classes of short-lived signaling proteins.[28,38] Germ cell apoptosis after cryptorchid stress involves genes for various factors, such as Bcl-2 family proteins, p53, and caspases;[39–44] however, the impact of the ubiquitin system on the regulatory mechanisms of germ cell apoptosis is not fully understood. In a previous study, we used *gad* mice, which lack UCH-L1 expression, to show that neural cell apoptosis is suppressed after ischemic retinal injury *in vivo*.[17] These results suggest that UCH-L1 is involved in apoptosis-inducing pathways after stress. UCH-L1 and UCH-L3 are highly similar in sequence; however, UCH-L3 is expressed ubiquitously,[7] whereas UCH-L1 is selectively expressed in neurons and testes/ovaries.[8,9] We recently demonstrated that the expression of these UCH isozymes is differentially and developmentally regulated during spermatogenesis, and that UCH-L1 and UCH-L3 likely have distinct functions during different developmental phases.[18]

To understand the pathophysiological roles of UCH-L1 and UCH-L3 *in vivo*, two mutant mice, *Uchl3* knockout and *gad* mice, were examined after cryptorchid injury. The cryptorchid testes of the two mutant mice had fundamental differences after injury, in that testes of *Uchl3* knockout mice showed profound apoptosis-mediated germ cell loss, whereas *gad* mice were relatively resistant to injury (Figures 3 and 4). In addition, cryptorchid testes of *Uchl3* knockout mice showed greater testicular atrophy and germ cell loss than wild-type mice.

There are several proposed mechanisms for germ cell loss after experimental cryptorchidism.[21–23,45] The tumor suppressor protein, p53, is highly expressed in the testis and regulates both cell proliferation and apoptosis.[23,28,37] A role for p53 in experimental cryptorchidism has been demonstrated convincingly. The higher temperature of the testis caused by cryptorchidism induces p53-mediated apoptosis in the testis, and p53 overexpression results in increased germ cell apoptosis and decreased spermatozoa production.[23,46] In addition to p53, the Bcl-2 family and IAP (inhibitor of apoptosis protein) family are other major classes of intracellular apoptosis regulators.[47,48] The Bcl-2 family can be divided into anti-apoptotic members, such as Bcl-2, Bcl-xL, and Bcl-w, and proapoptotic members, such as Bax and Bak.[49] It has been suggested that the ratio of proapoptotic to anti-apoptotic Bcl-2 family members is important in determining whether a cell will undergo apoptosis.[49] A major function of the Bcl-2 family members appears to be the regulation of mitochondrial events, such as the release of proapoptotic factors.[50] The IAP family inhibits apoptosis primarily by inactivating and degrading proapoptotic proteins.[51] XIAP, a member of IAP family, can bind to and inhibit the proteinase activity of cellular caspase-3 and caspase-9, and thereby block the apoptotic process.[44,52,53]

With regard to cryptorchid injury, the balance between the expression of apoptosis-inducing and apoptosis-protecting proteins constitutes one possible mechanism underlying the observed germ cell apoptosis and protection from apoptosis in *Uchl3* knockout and *gad* mice, respectively. In *gad* mice, cryptorchid injury caused a large increase in the anti-apoptotic proteins Bcl-2, Bcl-xL, and XIAP, consistent with our previous report using retina.[17]

In addition, the expression levels of the prosurvival proteins pCREB and BDNF also increased in *gad* mice. Consistent with these results, caspase-3 expression was suppressed in *gad* mice. Cryptorchid testes of *Uchl3* knockout mice showed slightly increased expression of the apoptotic proteins p53, Bax, and caspase-3 after injury, although similar increases were also observed in wild-type control mice. In total, these results suggest that UCH-L1 plays a role in balancing the expression of apoptosis-inducing and apoptosis-protecting proteins. In contrast, UCH-L3 seems to resist germ cell apoptosis after cryptorchid injury.

Recent studies demonstrate that many molecules in the cellular apoptosis machinery, such as p53,[39,41] Bcl-2 family,[42,43,54] XIAP,[52] and caspase[44] members, are targets for ubiquitination.[28] This suggests that ubiquitination is one of the major mechanisms by which apoptotic cell death is regulated. UCH-L1 has been suggested to associate with monoubiquitin,[13] and the monoubiquitin pool is reduced in *gad* mice relative to wild-type mice. Protection from cryptorchid injury was reported in testes of mice expressing a mutant K48R ubiquitin,[22] suggesting that ubiquitin plays a critical role in processing or modulating testicular insults. Normally, damaged proteins are polyubiquitinated and degraded via the ubiquitin-proteasome system; however, if damaged proteins are not degraded as easily when monoubiquitin is either depleted or mutated, then germ cell death could be delayed.[17,22] Our results with the *gad* mouse suggest that ubiquitin induction plays a critical role in regulating cell death during cryptorchid injury-mediated germ cell apoptosis.

Uchl3 knockout mice exhibit severe retinal degeneration, suggesting that the UCH-L3-mediated ubiquitin pathway is involved in retinal homeostasis.[55] In the cryptorchid testes of *Uchl3* knockout mice, however, the profound testicular weight reduction and germ cell apoptosis after injury cannot be explained by ubiquitin induction alone. Our present results show that *Uchl3* knockout and wild-type mice have similar ubiquitin expression level in the testes, suggesting that UCH-L3 has another nonhydrolase activity in the ubiquitin-proteasome system. UCH-L3 also binds and cleaves the C-terminus of the ubiquitin-like protein, Nedd8.[14,56] This activity is unique to UCH-L3 because UCH-L1 does not cleave Nedd8. Thus, UCH-L3 appears to have dual affinities for ubiquitin and Nedd8. Our present results show that Nedd8 is strongly induced in scrotal testes of *Uchl3* knockout mice compared with those of wild-type mice (Figure 7). Cryptorchid testes of both *Uchl3* knockout and wild-type mice showed Nedd8 induction after injury, although the induction was higher in *Uchl3* knockout mice. These observations suggest that UCH-L3 may function as a deneddylating enzyme[16] *in vivo*, although further studies are necessary to clarify whether UCH-L3 interacts with Nedd8 during spermatogenesis.

In the present study, we demonstrate apparent reciprocal functions for the two deubiquitinating enzymes, UCH-L1 and UCH-L3, with respect to mediating injury after experimental cryptorchidism (Figure 8). Our results advance our understanding of the role of the ubiquitin-proteasome system in regulating apoptosis, and provide a unique opportunity for effective therapeutic intervention.

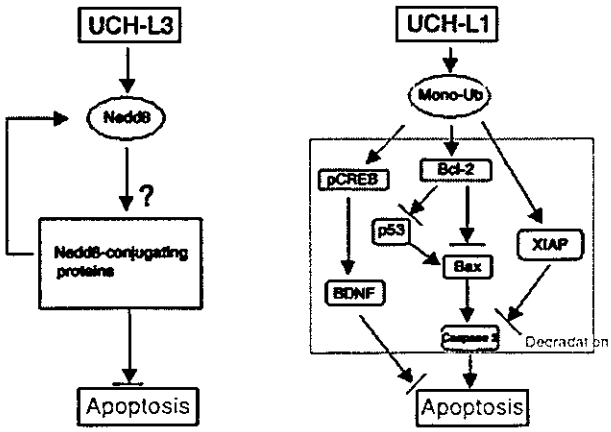

Figure 8. Differential function of the two UCH isozymes in response to experimental cryptorchidism. UCH-L3 has specificity for Nedd8. Cryptorchid injury results in protein damage and the accumulation of Nedd8-conjugated proteins. The accumulation of Nedd8-conjugated proteins in *Uchl3* knockout mice may contribute to profound germ cell loss via apoptosis. Hence, UCH-L3 might function as an anti-apoptotic regulator. UCH-L1 is involved in the maintenance of monoubiquitin levels. A deficiency in monoubiquitin results in delayed polyubiquitination and the accumulation of short-lived proteins after cryptorchid injury. Hence, UCH-L1 may function as a regulator of apoptosis.

Acknowledgments

We thank Dr. S.M. Tilghman for providing *Uchl3* knockout mice, H. Kikuchi for technical assistance with tissue sections, and M. Shikama for the care and breeding of animals.

References

1. Weissman AM: Themes and variations on ubiquitylation. Nat Rev Mol Cell Biol 2001, 2:169–178
2. Ciechanover A: The ubiquitin-proteasome pathway: on protein death and cell life. EMBO J 1998, 17:7151–7160
3. Pickart CM, Rose IA: Ubiquitin carboxyl-terminal hydrolase acts on ubiquitin carboxyl-terminal amides. J Biol Chem 1985, 260:7903–7910
4. Baker RT, Tobias JW, Varshavsky A: Ubiquitin-specific proteases of Saccharomyces cerevisiae. Cloning of UBP2 and UBP3, and functional analysis of the UBP gene family. J Biol Chem 1992, 267:23364–23375
5. Osawa Y, Wang YL, Osaka H, Aoki S, Wada K: Cloning, expression, and mapping of a mouse gene, Uchl4, highly homologous to human and mouse Uchl3. Biochem Biophys Res Commun 2001, 283:627–633
6. Kurihara LJ, Kikuchi T, Wada K, Tilghman SM: Loss of Uch-L1 and Uch-L3 leads to neurodegeneration, posterior paralysis and dysphagia. Hum Mol Genet 2001, 10:1963–1970
7. Kurihara LJ, Semenova E, Levorse JM, Tilghman SM: Expression and functional analysis of Uch-L3 during mouse development. Mol Cell Biol 2000, 20:2498–2504
8. Saigoh K, Wang YL, Suh JG, Yamanishi T, Sakai Y, Kiyosawa H, Harada T, Ichihara N, Wakana S, Kikuchi T, Wada K: Intragenic deletion in the gene encoding ubiquitin carboxy-terminal hydrolase in gad mice. Nat Genet 1999, 23:47–51
9. Kon Y, Endoh D, Iwanaga T: Expression of protein gene product 9.5, a neuronal ubiquitin C-terminal hydrolase, and its developing change in Sertoli cells of mouse testis. Mol Reprod Dev 1999, 54:333–341
10. Wilkinson KD, Deshpande S, Larsen CN: Comparisons of neuronal (PGP 9.5) and non-neuronal ubiquitin C-terminal hydrolases. Biochem Soc Trans 1992, 20:631–637
11. Liu Y, Fallon L, Lashuel HA, Liu Z, Lansbury Jr PT: The UCH-L1 gene

encodes two opposing enzymatic activities that affect alpha-synuclein degradation and Parkinson's disease susceptibility. Cell 2002, 111:209–218
12. Liu Y, Lashuel HA, Choi S, Xing X, Case A, Ni J, Yeh LA, Cuny GD, Stein RL, Lansbury Jr PT: Discovery of inhibitors that elucidate the role of UCH-L1 activity in the H1299 lung cancer cell line. Chem Biol 2003, 10:837–846
13. Osaka H, Wang YL, Takada K, Takizawa S, Setsuie R, Li H, Sato Y, Nishikawa K, Sun YJ, Sakurai M, Harada T, Hara Y, Kimura I, Chiba S, Namikawa K, Kiyama H, Noda M, Aoki S, Wada K: Ubiquitin carboxy-terminal hydrolase L1 binds to and stabilizes monoubiquitin in neuron. Hum Mol Genet 2003, 12:1945–1958
14. Wada H, Kito K, Caskey LS, Yeh ET, Kamitani T: Cleavage of the C-terminus of NEDD8 by UCH-L3. Biochem Biophys Res Commun 1998, 251:688–692
15. Hemelaar J, Borodovsky A, Kessler BM, Reverter D, Cook J, Kolli N, Gan-Erdene T, Wilkinson KD, Gill G, Lima CD, Ploegh HL, Ovaa H: Specific and covalent targeting of conjugating and deconjugating enzymes of ubiquitin-like proteins. Mol Cell Biol 2004, 24:84–95
16. Gong L, Kamitani T, Millas S, Yeh ET: Identification of a novel isopeptidase with dual specificity for ubiquitin- and NEDD8-conjugated proteins. J Biol Chem 2000, 275:14212–14216
17. Harada T, Harada C, Wang YL, Osaka H, Amanai K, Tanaka K, Takizawa S, Setsuie R, Sakurai M, Sato Y, Noda M, Wada K: Role of ubiquitin carboxy terminal hydrolase-L1 in neural cell apoptosis induced by ischemic retinal injury in vivo. Am J Pathol 2004, 164:59–64
18. Kwon J, Wang YL, Setsuie R, Sekiguchi S, Sakurai M, Sato Y, Lee WW, Ishii Y, Kyuwa S, Noda M, Wada K, Yoshikawa Y: Developmental regulation of ubiquitin C-terminal hydrolase isozyme expression during spermatogenesis in mice. Biol Reprod 2004, 71:515–521
19. Boekelheide K, Hall SJ: 2,5-Hexanedione exposure in the rat results in long-term testicular atrophy despite the presence of residual spermatogonia. J Androl 1991, 12:18–26
20. Ohta Y, Nishikawa A, Fukazawa Y, Urushitani H, Matsuzawa A, Nishina Y, Iguchi T: Apoptosis in adult mouse testis induced by experimental cryptorchidism. Acta Anat (Basel) 1996, 157:195–204
21. Yin Y, Hawkins KL, DeWolf WC, Morgentaler A: Heat stress causes testicular germ cell apoptosis in adult mice. J Androl 1997, 18:159–165
22. Rasoulpour RJ, Schoenfeld HA, Gray DA, Boekelheide K: Expression of a K48R mutant ubiquitin protects mouse testis from cryptorchid injury and aging. Am J Pathol 2003, 163:2595–2603
23. Yin Y, DeWolf WC, Morgentaler A: Experimental cryptorchidism induces testicular germ cell apoptosis by p53-dependent and -independent pathways in mice. Biol Reprod 1998, 58:492–496
24. Peltola V, Huhtaniemi I, Ahotupa M: Abdominal position of the rat testis is associated with high level of lipid peroxidation. Biol Reprod 1995, 53:1146–1150
25. Ahotupa M, Huhtaniemi I: Impaired detoxification of reactive oxygen and consequent oxidative stress in experimentally cryptorchid rat testis. Biol Reprod 1992, 46:1114–1118
26. Morimoto RI, Santoro MG: Stress-inducible responses and heat shock proteins: new pharmacologic targets for cytoprotection. Nature Biotechnol 1998, 16:833–838
27. Wojcik C: Proteasomes in apoptosis: villains or guardians? Cell Mol Life Sci 1999, 56:908–917
28. Yang Y, Yu X: Regulation of apoptosis: the ubiquitous way. EMBO J 2003, 17:790–799
29. Kwon J, Kikuchi T, Setsuie R, Ishii Y, Kyuwa S, Yoshikawa Y: Characterization of the testis in congenitally ubiquitin carboxy-terminal hydrolase-1 (Uch-L1) defective (gad) mice. Exp Anim 2003, 52:1–9
30. Taylor CT, Furuta GT, Synnestvedt K, Colgan SP: Phosphorylation-dependent targeting of cAMP response element binding protein to the ubiquitin/proteasome pathway in hypoxia. Proc Natl Acad Sci USA 2000, 97:12091–12096
31. Park C, Choi WS, Kwon H, Kwon YK: Temporal and spatial expression of neurotrophins and their receptors during male germ cell development. Mol Cells 2001, 12:360–367
32. Finkbeiner S: CREB couples neurotrophin signals to survival messages. Neuron 2000, 25:11–14
33. Selvakumaran M, Lin HK, Miyashita T, Wang HG, Krajewski S, Reed JC, Hoffman B, Liebermann D: Immediate early up-regulation of bax expression by p53 but not TGF beta 1: a paradigm for distinct apoptotic pathways. Oncogene 1994, 9:1791–1798
34. Liu L, Cavanaugh JE, Wang Y, Sakagami H, Mao Z, Xia Z: ERK5 activation of MEF2-mediated gene expression plays a critical role in BDNF-promoted survival of developing but not mature cortical neurons. Proc Natl Acad Sci USA 2003, 100:8532–8537
35. Matsui Y: Regulation of germ cell death in mammalian gonads. APMIS 1998, 106:142–148
36. Gosden R, Spears N: Programmed cell death in the reproductive system. Br Med Bull 1997, 53:644–661
37. Print CG, Loveland KL: Germ cell suicide: new insights into apoptosis during spermatogenesis. Bioessays 2000, 22:423–430
38. Lee JC, Peter ME: Regulation of apoptosis by ubiquitination. Immunol Rev 2003, 193:39–47
39. Haupt Y, Maya R, Kazaz A, Oren M: Mdm2 promotes the rapid degradation of p53. Nature 1997, 387:296–299
40. Oren M: Regulation of the p53 tumor suppressor protein. J Biol Chem 1999, 274:36031–36034
41. Ryan KM, Phillips AC, Vousden KH: Regulation and function of the p53 tumor suppressor protein. Curr Opin Cell Biol 2001, 13:332–337
42. Dimmeler S, Breitschopf K, Haendeler J, Zeiher AM: Dephosphorylation targets Bcl-2 for ubiquitin-dependent degradation: a link between the apoptosome and the proteasome pathway. J Exp Med 1999, 189:1815–1822
43. Marshansky V, Wang X, Bertrand R, Luo H, Duguid W, Chinnadurai G, Kanaan N, Vu MD, Wu J: Proteasomes modulate balance among proapoptotic and antiapoptotic Bcl-2 family members and compromise functioning of the electron transport chain in leukemic cells. J Immunol 2001, 166:3130–3142
44. Suzuki Y, Nakabayashi Y, Takahashi R: Ubiquitin-protein ligase activity of X-linked inhibitor of apoptosis protein promotes proteasomal degradation of caspase-3 and enhances its anti-apoptotic effect in Fas-induced cell death. Proc Natl Acad Sci USA 2001, 98:8662–8667
45. Yin Y, Stahl BC, DeWolf WC, Morgentaler A: P53 and Fas are sequential mechanisms of testicular germ cell apoptosis. J Androl 2002, 23:64–70
46. Ohta H, Aizawa S, Nishimune Y: Functional analysis of the p53 gene in apoptosis induced by heat stress or loss of stem cell factor signaling in mouse male germ cells. Biol Reprod 2003, 68:2249–2254
47. Beumer TL, Roepers-Gajadien HL, Gademan IS, Lock TM, Kal HB, De Rooij DG: Apoptosis regulation in the testis: involvement of Bcl-2 family members. Mol Reprod Dev 2000, 56:353–359
48. Oldereid NB, Angelis PD, Wiger R, Clausen OP: Expression of Bcl-2 family proteins and spontaneous apoptosis in normal human testis. Mol Hum Reprod 2001, 7:403–408
49. Borner C: The Bcl-2 protein family: sensors and checkpoints for life-or-death decisions. Mol Immunol 2003, 39:615–647
50. Yamamoto CM, Sinha Hikim AP, Huynh PN, Shapiro B, Lue Y, Salameh WA, Wang C, Swerdloff RS: Redistribution of Bax is an early step in an apoptotic pathway leading to germ cell death in rats, triggered by mild testicular hyperthermia. Biol Reprod 2000, 63:1683–1690
51. Deveraux QL, Reed JC: IAP family proteins—suppressors of apoptosis. Genes Dev 1999, 13:239–252
52. Yang Y, Fang S, Jensen JP, Weissman AM, Ashwell JD: Ubiquitin protein ligase activity of IAPs and their degradation in proteasomes in response to apoptotic stimuli. Science 2000, 288:874–877
53. Deveraux QL, Roy N, Stennicke HR, Van Arsdale T, Zhou Q, Srinivasula SM, Alnemri ES, Salvesen GS, Reed JC: IAPs block apoptotic events induced by caspase-8 and cytochrome c by direct inhibition of distinct caspases. EMBO J 1998, 17:2215–2223
54. Li B, Dou QP: Bax degradation by the ubiquitin/proteasome-dependent pathway: involvement in tumor survival and progression. Proc Natl Acad Sci USA 2000, 97:3850–3855
55. Semenova E, Wang X, Jablonski MM, Levorse J, Tilghman SM: An engineered 800 kilobase deletion of Uchl3 and Lmo7 on mouse chromosome 14 causes defects in viability, postnatal growth and degeneration of muscle and retina. Hum Mol Genet 2003, 12:1301–1312
56. Dil Kuazi A, Kito K, Abe Y, Shin RW, Kamitani T, Ueda N: NEDD8 protein is involved in ubiquitinated inclusion bodies. J Pathol 2003, 199:259–266

Journal of Neuroscience Research 72:211–217 (2003)

Growth Arrest of PC12 Cells by Nerve Growth Factor Is Dependent on the Phosphatidylinositol 3-Kinase/Akt Pathway Via p75 Neurotrophin Receptor

Hisanori Ito, Hiroshi Nomoto,* and Shoei Furukawa
Laboratory of Molecular Biology, Gifu Pharmaceutical University, Gifu, Japan

We recently isolated mutant PC12 cell clones (PC84 cells) by transfection of PC12 cells with nerve growth factor (NGF) cDNA. These cells secreted active NGF and extended short processes, but proliferated faster than the parental PC12 cells. Because the expression level of p75, a low-affinity receptor for NGF, was significantly low, we suspected that NGF signaling via p75 was necessary for the growth arrest of the PC12 cells, and this was shown to be the case by repressing p75 function in PC12 cells. In this study, we examined the downstream signaling of p75, which would ultimately evoke the growth arrest. NGF is known to induce rapid phosphorylation of MAP kinase and Akt in PC12 cells, whereas in PC84 cells, MAP kinase was phosphorylated but the phosphorylation level of Akt was very low under the serum-free condition. This finding suggested that the low expression level of p75 in PC84 cells was the reason for the low Akt activation. Because Akt is known to be activated via phosphatidylinositol (PI) 3-kinase, we treated PC12 cells with a PI3-kinase inhibitor, Wortmannin, and found these cells did not cease proliferation in the presence of NGF. Furthermore, anti-p75 neutralizing antibody reduced NGF-induced phosphorylation of Akt in PC12 cells under the serum-free condition. Because we had already shown that PC12 cells treated with anti-p75 neutralizing antibody did not cease proliferation in the presence of NGF, these results suggest that NGF activates Akt via p75, which is necessary for the NGF-induced growth arrest of PC12 cells.

Key words: growth arrest; Akt; PC12; p75; NGF

Neurotrophins are a family of structurally related secretory proteins involved in survival, development, and death of specific populations of neuronal and non-neuronal cells. Nerve growth factor (NGF) is the best-characterized member of this family. Two types of cell-surface receptors, TrkA and p75, are known to initiate the signal transduction systems that mediate the diverse biological functions of NGF (Lewin and Barde, 1996). The major effects of NGF on neuronal cells include the promotion of differentiation and survival of the cells. PC12 cells undergo transient proliferation followed by growth arrest and subsequent differentiation in response to NGF (Rudkin et al., 1989). NGF activates multiple signaling pathways via autophosphorylation of TrkA, including Ras, MAP kinase, phosphatidylinositol (PI) 3-kinase, and phospholipase C-γ (Ohmichi et al., 1992; Obermeier et al., 1993; Loeb et al., 1994). Several studies have shown that neuronal differentiation including neurite outgrowth could be induced by Ras/MAP kinase and PI3-kinase (Robbins et al., 1992; Kimura et al., 1994; Pang et al., 1995; Jackson et al., 1996). On the other hand, NGF-induced growth arrest in the process of neuronal differentiation is known to be accompanied by a change in the expression of cyclin, cyclin-dependent kinase (Cdk), and Cdk inhibitor (Dobashi et al., 1995; Yan and Ziff, 1995), but it is not clear how the expression of these cell cycle related proteins is controlled by NGF.

PI3-kinase is activated by a variety of mitogenic factors (Franke et al., 1995; Alessi et al., 1996) and mediates the main pathway for neuronal cell survival (Dudek et al., 1997; Crowder and Freeman, 1998). The activated PI3-kinase increases phosphatidylinositol 3,4,5-trisphosphate, which then recruits phosphoinositide-dependent kinase-1 and Akt serine/threonine kinase. Phosphorylation of Akt on threonine 308 by phosphoinositide-dependent kinase-1, followed by autophosphorylation on serine 473 activates Akt (Bellacosa et al., 1998; Toker and Newton, 2000). The enzyme then phosphorylates downstream substrates that include Bad, Caspase-9, IκB kinase, and glycogen synthase kinase-3 (Cross et al., 1995; del Peso et al., 1997).

The physiological function of p75 is suggested to be the regulatory activation and signaling of the Trk receptor (Barker and Shooter, 1994; Rydén et al., 1997; Bibel et

*Correspondence to Hiroshi Nomoto, Laboratory of Molecular Biology, Gifu Pharmaceutical University, Mitahora-Higashi, Gifu, Japan.
E-mail: hnomoto@gifu-pu.ac.jp

Received 15 October 2002; Revised 2 December 2002; Accepted 5 December 2002

Published online 6 February 2003 in Wiley InterScience (www.interscience.wiley.com). DOI: 10.1002/jnr.10564

al., 1999) and Trk-independent signal transduction pathways involving sphingomyelinase (Dobrowsky et al., 1994), nuclear factor-κB (Carter et al., 1996), and JNK (Casaccia-Bonnefil et al., 1996). Several studies have shown that NGF binding to p75 initiated a cell death cascade in some cell types (Barrett and Bartlett, 1994; Casaccia-Bonnefil et al., 1996; Frade and Barde, 1999). The details of the p75 function, however, especially its role in NGF-induced differentiation, are not clear.

Mutant PC12 cell clones, PC84 cells, were isolated previously by cloning growing cells after transfection of PC12 cells with NGF cDNA (Ito et al., 2002). These cells secreted active NGF and showed differentiated character; i.e., they extended short processes and expressed a high level of acetylcholinesterase activity and neurofilament M; however, these cells continued growing despite the fact that they were secreting active NGF. This character of PC84 cells presented an exquisite contrast to the parental PC12 cells, which cease proliferation and extend long processes when treated with NGF or are transfected with NGF cDNA. The most probable reason for this characteristic of PC84 cells was the low expression level of p75; the expression level of TrkA in PC84 cells was comparable to the parental PC12 cells, whereas that of p75 was significantly low. The involvement of p75 in the growth arrest was then confirmed by suppressing p75 activity of PC12 cells with the antisense oligonucleotide of p75 or with anti-p75 neutralizing antibody. The treated cells did not cease proliferation in the presence of NGF with the morphology having short processes. Because inhibition of TrkA by K252a diminished the short processes of PC84 cells, NGF signaling via TrkA affected mainly the differentiation character of PC12 cells, and the additional signaling via p75 was necessary for the growth arrest of the cells.

To unveil the relationship between signaling via p75 and the growth arrest of PC12 cells, we examined the intracellular signaling in PC84 cells. We found the phosphorylation level of Akt to be very low in PC84 cells under serum-free conditions. Moreover, PC12 cells treated with the PI3-kinase inhibitor Wortmannin did not cease proliferation in the presence of NGF, and NGF-induced phosphorylation of Akt in PC12 cells was reduced by the treatment with anti-p75 neutralizing antibody. All these results suggested that the low expression level of p75 in PC84 cells was responsible for the low Akt activation and such activation was necessary for the NGF-induced growth arrest of PC12 cells.

MATERIALS AND METHODS

Cell Culture

PC12 and PC84 cells were maintained in Dulbecco's modified Eagle's medium supplemented with 10% heat-inactivated horse serum and 5% heat-inactivated fetal bovine serum. The morphological study was conducted with collagen-coated dishes (Nomoto et al., 2000).

Preparation of NGF

Mouse NGF (β type) was purified by chromatography from 7S NGF isolated from adult male mouse submaxillary glands (Furukawa et al., 1983). The purity was checked by SDS-PAGE and no protein contaminants were detected.

Western Blotting

Cells were washed three times with ice-cold Tris-buffered saline (TBS; 10 mM Tris, pH 7.4, containing 0.15 M NaCl), and lysed with lysis buffer (20 mM Tris-HCl, pH 7.4, containing 1% Nonidet P-40, 1% sodium deoxycholate, 0.1% SDS, 0.15 M NaCl, 1% aprotinin, 10 μg/ml leupeptin, 50 mM sodium fluoride, 1 mM sodium orthovanadate, and 1 mM phenylmethylsulfonyl fluoride). The lysates were centrifuged for 20 min at 12,000 rpm, and the protein concentration of the supernatants was determined with a BCA Protein Assay Kit (Pierce, Rockford, IL). Western blotting was carried out as described previously (Ito et al., 2002) by using anti-phospho-Akt (Ser473) antibody, anti-Akt antibody, anti-phospho-p44/42 MAP kinase antibody, and anti-p44/42 MAP kinase antibody (New England Biolabs, Hertfordshire, UK). In this study, biotinylated anti-rabbit IgG antibody (Vector Laboratories, Burlingame, CA) was used as a second antibody (incubation time, 2 hr). Finally, membranes were incubated with avidin-biotinylated peroxidase complexes (Vector Laboratories) for 1 hr, and peroxidase activity was visualized with Tris-HCl, pH 7.4, containing 0.2% diaminobenzidine tetrahydrochloride (Dojindo Laboratories, Kumamoto, Japan), 0.003% (v/v) H_2O_2, and 0.6% (w/v) nickel ammonium sulfate.

Immunoprecipitation

Cells were washed three times with ice-cold TBS and lysed with the lysis buffer as specified in the Western blotting section. The lysates were centrifuged for 20 min at 12,000 rpm and the protein concentration of the supernatants was determined. The cell lysates then were incubated overnight at 4°C with anti-Trk antibody (Santa Cruz Biotech, Santa Cruz, CA) followed by incubation with Protein A-Sepharose beads (Amersham Biosciences, Piscataway, NJ) for 1 hr at 4°C. Thereafter, the pellet was collected, washed five times with lysis buffer, and boiled in the sample buffer for SDS-PAGE. Phosphorylated TrkA was detected by Western blotting with anti-phosphotyrosine antibody (Upstate Biotechnology, Lake Placid, NY).

Repression of P75 with Anti-P75 Antibody

PC12 cells were incubated with control mouse-IgG or anti-p75 antibody (Oncogene Research Products, San Diego, CA) (1 μg/ml) for 1 hr. NGF was added and the cells were incubated for 5 min. Phosphorylation of MAP kinase and Akt was assessed by Western blotting.

RESULTS

Activation of MAP Kinase and Akt in PC84 Cells

Our previous study showed that PC84 cells, which were derived from PC12 cells, kept proliferating in the presence of NGF, and suggested that the low expression level of p75 in PC84 cells was responsible for it. To clarify